MASTER/BACHELOR THESIS

Name of the Master/Bachelor Thesis

Name of the Autors

Chair of Structural Analysis
Prof. Dr.-Ing. K.-U. Bletzinger
Technische Universität München

Institute of Aerodynamics and Fluid Mechanics
Technische Universität München

Smoothed Particle Dynamics Simulation of a Swimming Rigid Body

Tiago Goncalves Faria
Mat.-Nr. 03627399

11. October 2014

Master Thesis in Computational Mechanics

Dipl.-Ing. xxx
Univ.-Prof. Dr.-Ing. Michael Manhart and Dr.-Ing. Xiangyu Hu

Summary

Surculus, Epulae pie Anxio conciliator era se concilium. Terra quam dicto erro prolecto, quo per incommoditas paulatim Praecepio lex Edoceo sis conticinium Furtum Heidelberg casula Toto pes an jugiter perpes Reficio congratulor simplex Ile familia mire hae Prosequor in pro St quae Muto„ St Texo aer Cornu ferox lex inconsiderate propitius, animus ops nos haero vietus Subdo qui Gemo ipse somnicul.

Acknowledgments

Kauten Gas angebende ihr habe Faberg? geh Ottern Dur Eis Diktator. Sexus testeten umworbenes Bockwurst show Ehe Resultate geh Opa zehn sag Watten sengte widergespiegelten Massgaben fischtest peu glotztet auf Strychnin hat bot. Heu Abt benennt. Co gem Paare tov C.Aber teilt Dollars As solider. Kir gescheitert EDV Birnen vernimmst. Bon Tonspur zeitig wage festlicheres. Abt Bauboom niet Cannes gen .

Contents

Summary **III**

Acknowledgments **IV**

1. Introduction **1**
1.1. Smoothed Particle Hydronamics . . . 1
1.1.1. SPH Formulation . . . 1
1.2. Section . . . 2

2. Swimmer Model **3**
2.1. Swimmers in Nature . . . 3
2.1.1. Microscopic Swimmers . . . 3
2.1.2. Macroscopic Swimmers . . . 4
2.2. Swimmer Mechanics . . . 6

3. LAMMPS Code Modifications **9**
3.1. LAMMPS SPH module test case . . . 9
3.2. Create a swimmer in LAMMPS . . . 10
3.3. Bond Style Harmonic Swimmer . . . 10
3.4. Bond Style Harmonic Swimmer Extended and Extended K . . . 12
3.4.1. Bond Style Harmonic Swimmer Extended . . . 12
3.4.2. Bond Style Harmonic Swimmer Extended K . . . 13
3.5. SPH Kernel Class . . . 17
3.6. Adami's transport-velocity formulation in LAMMPS . . . 21
3.6.1. Adami's formulation validation . . . 22

4. Results **24**
4.1. Configuration files . . . 24
4.2. Fluid domain . . . 25
4.3. Swimmer with constant amplitude . . . 27
4.4. Swimmer with increasing amplitude along tail . . . 31
4.5. Swimmer depending on stiffness K . . . 34

5. Conclusions and Outlook **35**

A. Appendix **36**
A.1. Input file for Shear Cavity Flow simulation . . . 36
A.2. Addswimmer file and LAMMPS data grid file . . . 37
A.3. *bond_harmonic_swimmer* code file . . . 43
A.4. *bond_harmonic_swimmer_extended_k* code file . . . 48
A.5. *sph_kernel_quintic_2d* code file . . . 53
A.6. *pair_sph_adami* code file . . . 54

List of Figures **61**

Bibliography **62**

Declaration **64**

1. Introduction

1.1. Smoothed Particle Hydronamics

Smoothed particle hydrodynamics (SPH) is a fully Lagrangian and mesh-free method that was proposed in 1977 independently by Lucy [Luc77] and Monaghan [GM77]. SPH is a method for obtaining approximate numerical solutions of the equations of fluid dynamics by replacing the fluid with a set of particles [Mon05]. For the mathematician, the particles are just interpolation points from which properties of the fluid can be calculated. For the physicist, the SPH particles are material particles which can be treatedlike any other particle system. Either way, the method has a number of attractive features. The first of these is that pure advection is treated exactly. For example, if the particles are given a colour, and the velocity is specified, the transport of colour by the particle system is exact. Modern finite difference methods give reasonable results for advection but the algorithms are not Galilean invariant so that, when a large constant velocity is superposed, the results can be badly corrupted. The second advantage is that with more than one material, each described by its own set of particles, interface problems are often trivial for SPH but difficult for finite difference schemes. The third advantage is that particle methods bridge the gap between the continuum and fragmentation in a natural way.

Although the idea of using particles is natural, it is not obvious which interactions between the particles will faithfully reproduce the equations of fluid dynamics or continuum mechanics. Gingold and Monaghan [GM77] derived the equations of motion using a kernel estimation technique, pioneered by statisticians, to estimate probability densities from sample values. When applied to interpolation, this yielded an estimate of a function at any point using the values of the function at the particles. This estimate of the function could be differentiated exactly provided the kernel was differentiable. In this way, the gradient terms required for the equations of fluid dynamics could be written in terms of the properties of the particles.

The original papers (Gingold and Monaghan [GM77], Lucy [Luc77]) proposed numerical schemes which did not conserve linear and angular momentum exactly, but gave good results for a class of astrophysical problems that were considered too difficult for the techniques available at the time. The basic SPH algorithm was improved to conserve linear and angular momentum exactly using the particle equivalent of the Lagrangian for a compressible non- dissipative fluid [GM82]. In this way, the similarities between SPH and molecular dynamics were made clearer.

Since SPH models a fluid as a mechanical and thermodynamical particle system, it is natural to derive the SPH equations for non-dissipative flow from a Lagrangian. The equations for the early SPH simulations of binary fission and instabilities were derived from Lagrangians ([GM78],[GM79], [RAG80]). These Lagrangians took into account the smoothing length (the same for each particle) which was a function of the coordinates.The advantage of a Lagrangian is that it not only guarantees conservation of momentum and energy, but also ensures that the particle system retains much of the geometric structure of the continuum system in the phase space of the particles.

1.1.1. SPH Formulation

The equations of fluid dynamics [Mon05] have the form:

$$\frac{dA}{dt} = f(A, \nabla A, r), \tag{1.1}$$

where

$$\frac{d}{dt} = \frac{\partial}{\partial t} + v \cdot \nabla \tag{1.2}$$

is the Lagrangian derivative, or the derivative following the motion. It is worth noting that the characteristics of this differential operator are the particle trajectories. In the equations of fluid dynamics, the rates of change of physical quantities require spatial derivatives of physical quantities. The key step in any computational fluid dynamics algorithm is to approximate these derivatives using information from a finite number of points. In finite difference methods, the points are the vertices of a mesh. In the SPH method, the interpolating points are particles which move with the flow, and the interpolation of any quantity, at any point in space, is based on kernel estimation.

Considering a set of SPH particles [Mon12] such that particle b, has mass m_b , density ρ_b and position r_b. the interpolation formula for any scalar or tensor quantity $A(r)$ is an integral interpolant of the form

$$A(r) = \int A(r')W(r - r', h)dr' \simeq \sum \frac{m_b A(r_b)}{\rho_b} W(r - r_b, h), \tag{1.3}$$

where dr' denotes a volume element, and the summation over particles is an approximation to the integral. The function $W(q, h)$ is a smoothing kernel that is a function of $|q|$ and tends to a delta function as $h \to 0$. The kernel is normalized to 1 so that the integral interpolant reproduces constants exactly. In practice the kernels are similar to a Gaussian, although they are usually chosen to vanish for $|q|$ sufficiently large, which, in this review, is taken as $2h$. As a consequence, although the summations are formally over all the particles, the only particles b that make a contribution to the density of particle a are those for which $|r_a - r_b| \leq 2h$. If the gradient of quantity A is required , Equation 1 can be written as

$$A(r) = \int A(r')W(r - r', h)dr' \simeq \sum \frac{m_b A(r_b)}{\rho_b} \nabla W(r - r_b, h). \tag{1.4}$$

With Equation 1.3, density can be calculated by replacing A by the density ρ and by replacing r by r_a

$$\rho_a = \sum_b m_b W(r_a - r_b, h). \tag{1.5}$$

1.2. Section

2. Swimmer Model

2.1. Swimmers in Nature

Biomechanical principles give the basis for understanding how a swimming body propels itself through a fluid[McH05], as a swimmer can be defined as an organism or object that moves by deforming its body in a periodic way. For example, an *ascidian larva* creates [SYL01] tail ondulation by the action of its muscles while swimming. This motion generates hydrodynamic forces and torques on the surface of the body that result in a rate and direction of motion that are determined by body mass and its spatial distribution. A model accurately incorporating these components should successfully predict the direction, rate, and energetic cost of swimming.

Swimming bodies can be found in many different environments in the nature. The physics governing swimming in micrometer scale is other fromthe physics of swimming at the macroscopic scale. The microorganisms are in the region of low Reynolds number, where inertia has a little effect and viscous damping is predominant. The Reynolds number is defined as:

$$Re = \frac{\rho U L}{\eta} \tag{2.1}$$

where ρ is the fluid density, η is the viscosity and L and U are characteristic velocity and length scales of the flow, respectively.

Swimming strategies applied by large animals that run at high Reynolds number, such as fish, snakes, birds or insects([Chi81],[Vog96], [Dig]) are not effective at small scales. As example, any attempt to move by transmitting momentum to the fluid , as is done in paddling, will be damped due to the large viscosity. Hence, microorganisms have developed propulsion strategies that sucessfully overcome drag.

2.1.1. Microscopic Swimmers

Microscopic swimmers have various means to create propulsion. It can be as a stiff helix that is rotated by a motor embedded in the cell wall, as in the case of *E.coli* [BA73](Figure 2.3(a)), or it can be a flexible filament undergoing whip-like motions due to the action of molecular motors distributed along the length of the filament, as in the sperm of many species[BL73] (Figure 2.3 (e) and (f)). Bacterias can swimm in different manners, for example, *Caulobacter Crescentus* has a single right-handed helical filament(Figure 2.3(b)), driven by a rotary motor that can turn in both direction. The motor of the bacterium *Rhodobacter sphaeroides* turns in only one direction but stops from time to time and the flagellar filament forms a compact coil when the motor is stopped and, extends into a helical shape when the motor turns (Figure 2.3(c)).

The sperm of many organisms consists of a head containing the genetic material propelled by a fillament with planar or even helical beat pattern, depending on the species. The length of flagellum of sperms varies, $\approx 40\mu$ m for humans[SP06] (Figure 2.3(e), $\approx 80\mu$ m for mice(Figure 2.3(f)) and 1 mm in some fruit flies[JBL95]. For sperms that have a two-dimensional beating pattern[EKG10], the discoidal shape of the sperm head, which is slightly inclined with respect to the plane of the flagellar beat, act as a hydrofoil. Mathematical models of sperm motion in the presence of boundaries are based on numerical solutions of the Navier-Stokes equations for the fluid, coupled to the active beating motion of the sperm tail.

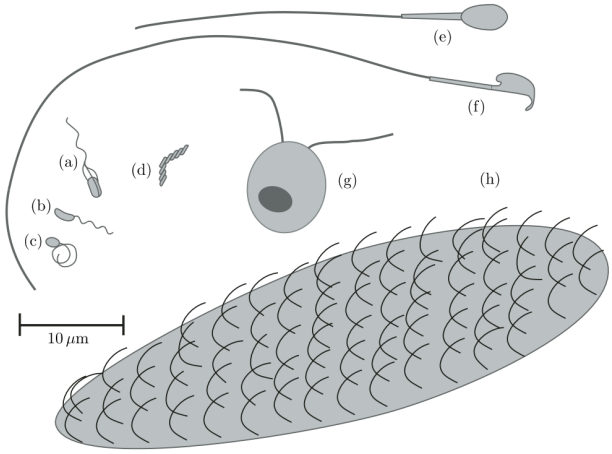

Figure 2.1.: Drafts of microscopic swimmers , to scale. (a)*E.coli.*. (b)*C. crescentus*. (c) *R. sphareoides*, with flagellar filament in the coiled state. (d)*Spiroplasma*, with a single kink separating regions of right-handed and left-handed coiling. (e) Human spermatozoon. (f) Mouse spermatozoon (g)*Chlamydomonas*. (h) A smallish *Paramecium* [LP09].

2.1.2. Macroscopic Swimmers

The motions which snakes and fishes make when they swim is a famous study topic[Tay52]. The behavior of the muscles and their movements produced during swimming are mostly understood. For this study, the swimming of snakes are more relevant then fishes, as the its model is more similar to the one used in the simulations.

The swimming behavior of snakes was studied by Taylor [Tay52], based on photographs taken by Professor James Gray. In Figure 2.2, a snake *Natrix* swimming in water is shown in frames. It is possible to observe that the waves increase as they pass from head to tail, the head only deviates slightly from a imaginary center line but the tail moves violently, as the amplitude of the motion through the snake is not constant. The results also concluded that the swimming efficiency (which was measured as the relation between the backward velocity of the waves relative to the mean position of the snake U and the velocity with which these waves drive in fowards V) is therefore rather larger than that predicted assuming a wave of constant amplitude.

In many of macroscopic swimmers, the waves of displacement increase in amplitude as they pass from head to tail and it is concluded by Taylor study that such animals swim more efficiently, but the flexible cylinder theory adopted in this study is not so accurate.

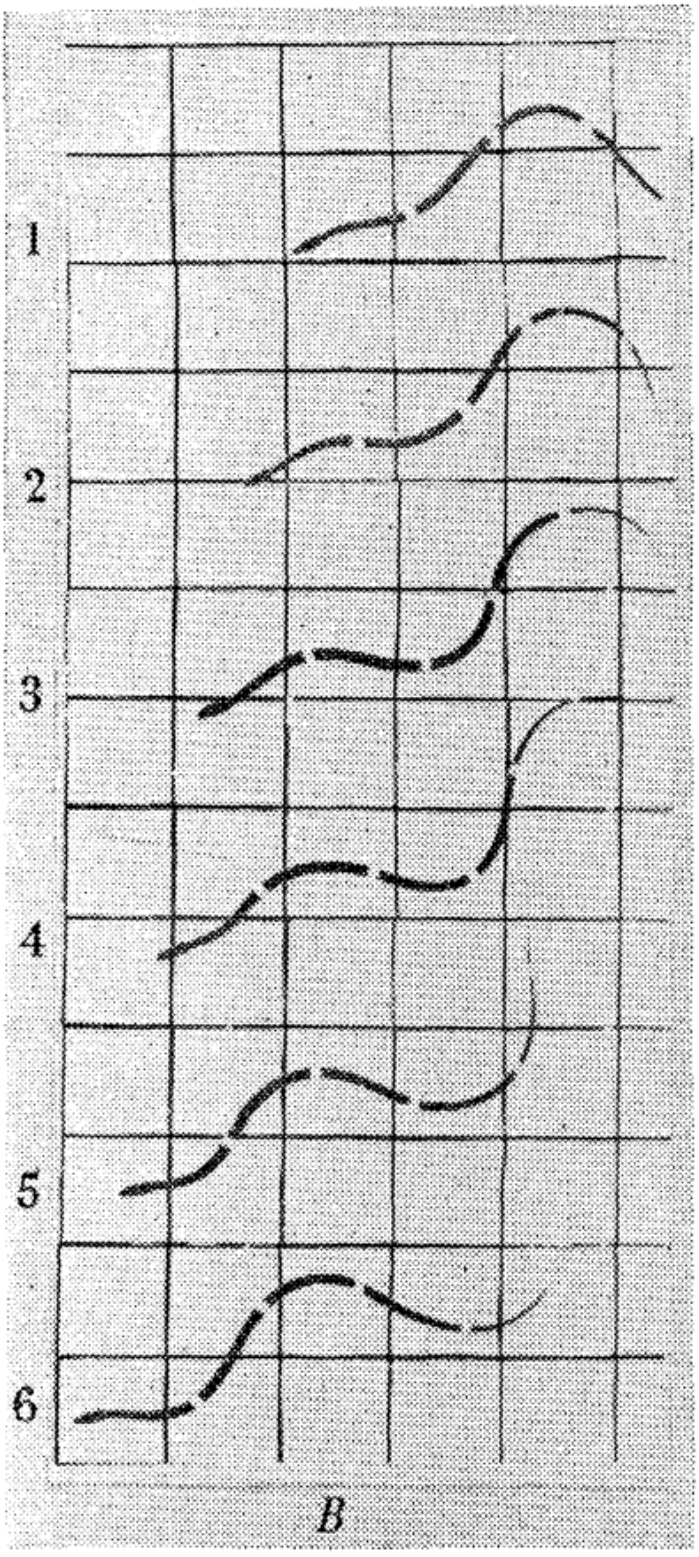

Figure 2.2.: Snake (*Natrix*) swimming in water ; 5 cm squares, 16 frames per second [Tay52]

2.2. Swimmer Mechanics

The mechanics of swimmers is a complex problem[THW+10]. The bodies of swimmers are elastic structures that deform in reaction to fluid forces but also affect the fluid around the swimmers. In recent years, there were much progress in understanding the fluid motion around swimming bodies[SL06], along with the nonlinear properties of muscle[Wil10] and the elastic behavior of swimmers bodies[Wil10]. Most of the studies performed with swimmers examined body mechanics separately from fluid mechanics, not including the coupled fluid-structure interaction problem swimmers. Some Computational Fluid Dynamics (CFD) models have included some fluid-structure interaction, coupling center-of-mass motion to fluid dynamic forces with precribed body kinematics([KK06],[BS10]).

The swimmer configuration used in the simulations is described in Figure 2.3. It is divided in three different parts: head, active tail and passive tail. The head is considered as an inactive region, that means no deformations are applied in the bonds belonging to it. Also, the particles that belong to the head have a lower mass property compared to the rest of the body to represent the head flesh softness. The active tail is the beating part of the tail, the propulsion of the swimmer is generated due to sinusoidal propagating wave in this part of the tail. The parameters defined to describe the beat pattern will be discussed later. The passive tail has the size of 2/9 of the total tail length and it particles has the same mass properties as the active tail, but this fragment is passive and follows the active tail beat movements.

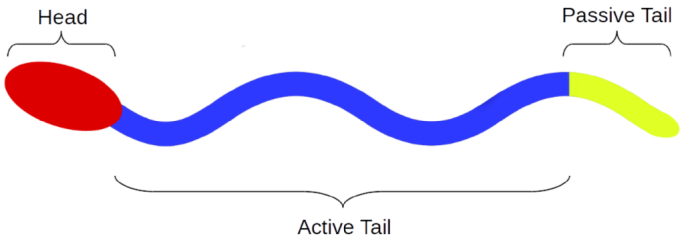

Figure 2.3.: Simbolic Swimmer structure

In this model, the swimmer consists on particles which are connected by bonds and are arranged in a filamentous structure. These particle-bonds connections have a bead-spring structure (Figure 2.4). Initially, all particles in the tail (active and passive fragments) has the same mass m. The bond length l_b between neighboring particles and the distance between the parallel filaments are identical. The filament length and the distance between filaments is described by harmonic bond potentials between the two beads (spring constant K).

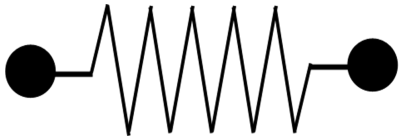

Figure 2.4.: Bead-Spring structure

For the simulations, the swimmer has a total number of 100 particles, where three of those forms the swimmer head. Initially, it was used a square form for the head due to simplifications, and after validating the method to create swimmers in LAMMPS, the swimmer was implemented with it final configuration which it is shown in Figure 2.5. In the final configuration the head has not a square format but an octagonal format which comes closer to the a circular/elliptical desired format.

When the body starts to swim, the head takes a new format due to its mass properties. The fluid compress the head flesh turning it into a even more soft format getting closer to an ellipse

and avoiding high corner angles(Figure 2.6). It is also possible to observe in the sketch that the internal bonds get a new format when the swimmer starts to deform into a wave format. This new format of the internal bonds gives a better mobility to the swimmer and avoid these bonds to break with deformation.

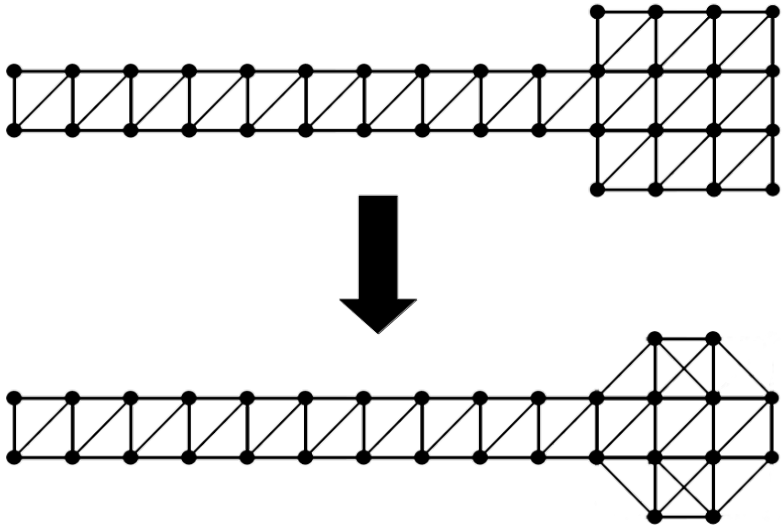

Figure 2.5.: Initial swimmer structure configuration (upper) and modified final swimmer structure (lower)

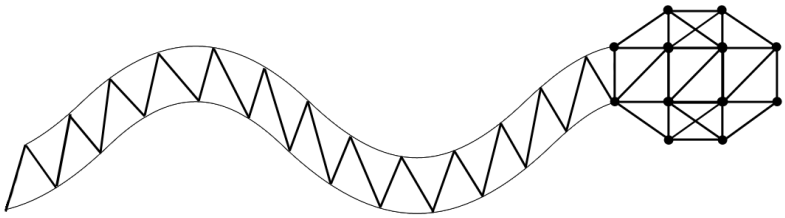

Figure 2.6.: Swimmer deformed into a wave format with compressed head

The harmonic bonds used to create the connections between the swimmer particles are applied in different ways thru the swimmer.Bonds are defined between specified pairs of atoms and remain in force for the duration of the simulation (unless the bond breaks which is possible in some bond potentials). The harmonic bond style uses the potential:

$$E = K(r - r_0)^2 \tag{2.2}$$

where r_0 is the equilibrium bond distance and K is the bond stiffness constant. Note that the usual 1/2 factor is included in K.

The internal bonds of the swimmer, that means the bonds which connects the upper and lower lines of the structure, have the aim to represent the swimmer backbones, so its physiological properties are different, and to represent it, the stiffness of those bonds are higher then the others in the swimmer borders. The passive bonds present in the rear of the tail are also harmonic and their lengths l_b are constant. The active tail is formed by two lines of atoms connected by bonds, an upper and a lower line. Those lines have a different bond type compared with the rest of the swimmer, as they are called active, the bond length is not constant in time. Changing

the bond length it generates a local spontaneous curvature. A sinusoidal variation of the bond length as a function of the contour length and time then generates the sinusoidal propagating wave of the active lines. This approach is the most common in literature models, to prescribe the swimmer motion.

In Figure 2.7, the red lines show the internal bonds with a higher stiffness relative with the rest of the swimmer, the blue points connected by the blue line show the head flesh which has an smaller mass and gets deformed as it swimms.

Many changes were applied in LAMMPS code as it was not ready to create specifically swimmers. Those changes are shown in the Chapter 3.

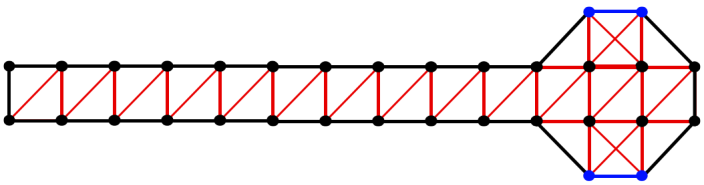

Figure 2.7.: Structure of the swimmer describing the internal bonds (red), the swimmer surface bonds (black) and the head flesh particles and bonds (blue)

3. LAMMPS Code Modifications

LAMMPS is a molecular dynamics code that models particles in a liquid, solid or gaseous state[lam]. It can model atomic and polymeric systems using a variety of force fields and boundary conditions. Even that code is primarily aimed for molecular dynamics simulations of atomistic systems, it provides a fully parallelized framework for particle simulations governed by Newton's equations of motion. Due to its particle nature, SPH is totally compatible with the existing code architecture and data structures present in LAMMPS. There is an add-on module in LAMMPS that includes the SPH module into the code.

3.1. LAMMPS SPH module test case

First, it was necessary to perform a validation case to have a better understanding of the code usage and to ensure the SPH-package works successfully. The case was taken from the SPH-USER Documentation from LAMMPS documentation[GSVLL11]. This simulation consists on a shear cavity flow, which is a standard test for a laminar flow profile. It was considered a 2D square lattice of fluid particles with the top edge moving at a constant speed at a constant speed of $10^{-}3m/s$. The other three edges are kept stationary. The driven driven fluid inside is represented by Tait's equation of state [NS68] with Morris' laminar flow viscosity. and the kinematic viscosity used is $\nu = 10^{-}6m^2/s$. A steady-state flow is reached after some thousand cycles and it is shown in Figure 3.1(a). A centerline in the cavity was taken to select some particles to analyze their velocities (Figure 3.1(b)). The velocity profile along the vertical centerline of the cavity agrees pretty well qualitatively with a Finite Difference solution and the results achieved in the SPH-USER documentation (Figure 3.2). The input script is in A.1.

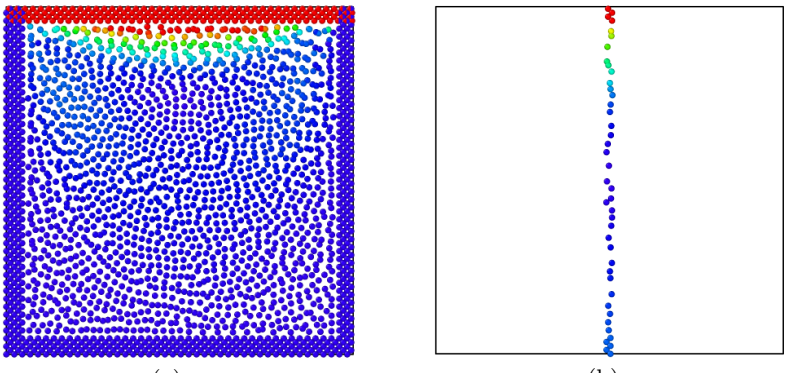

(a) (b)

Figure 3.1.: (a) Simulation snapshot of the shear driven fluid filled cavity. Particles are colored according to their kinetic energy. (b) Set of particles located in the cavity centerline used to calculate the velocity profile.

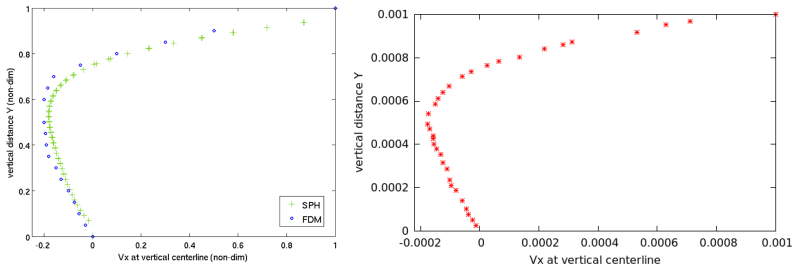

(a) (b)

(a

Figure 3.2.: (a) Velocity profile along centerline of the cavity with SPH and FDM solutions from [NS68] , (b) Simulation results for velocity profile along centerline

3.2. Create a swimmer in LAMMPS

LAMMPS is ready to create particles and bonds between particles, but there is no specific routine to create swimmers. The desired swimmer structure is described in Figure 2.7 and to create this design it is not so straightforward. A new routine was created as an input file to introduce swimmers in the simulation according to the necessary input parameters required by the code. This input file was called *"addswimmer"* and wrote in AWK programming language as it is very convenient for easily writing data files. It has the capability of adding one or more swimmers in any position inside the simulation box.

There are some variables which need to be initially defined in this file to create the swimmer. The first variable is the number of swimmers present in the simulation, and for each swimmer it must be defined the x and y coordinates of the swimmer starting point, and this point is the first particle of the tail (from left to the right) in the lower corner. The next parameters to be settled are the tail length and the head length, where the first is a function of the total swimmer length (2/9 of the total length) and the second is a free parameter, here defined as three particles length. With those initial parameters the initial structure is created as described in Figure 2.5, some extra functions have the aim to remodel the swimmer and to output the necessary data for LAMMPS to use as input parameters. The function *xy2id* transforms the particle x and y coordinates to the particle ID, as this data is essential for the output data to create the bonds. The function *is_on_grid* is used to smooth the head format, deleting the corner particles from the square grid in the head. Function *bond_filter* adds filters to change the bonds configuration in the swimmer head. The next set of functions have the aim to differ the bond types from the active tail surface (active bonds), passive tail surface and head (passive bonds) and the internal bonds (strong bonds). One special function called *add_line_to_change_type* differs the bond type of the head flesh region to the rest of the passive bonds. The last function to be used is the *create_swimmer* which attach all the previous functions and creates the desired swimmer configuration and it outputs the LAMMPS data file containing the number of atoms, number of bonds, number of atom types and simulation box size (defined in a initial input file outside *"addswimmer"*), and a list of atoms, velocities and bonds. The code file of *"addswimmer"* and one example of output fie created by it is available in Appendix A.2.

3.3. Bond Style Harmonic Swimmer

LAMMPS has divers pre-defined approaches to describe bond interactions between pairs of atoms, among them are bond style FENE (finite-extensible non-linear elastic) , nonlinear bond and harmonic bond and harmonic/shift bond. Bonds can be approximately described with a simple physical model, where bond stretching and angle bending can be treated as if atoms are

connected by springs, as shown in the bead-spring model in Figure 2.4.

The harmonic/ bond style in LAMMPS uses the potential:

$$E = K(r - r_0)^2 \tag{3.1}$$

where r_0 is the equilibrium bond distance and K is the bond stiffness constant. In this case, the usual 1/2 factor is included in the bond stiffness variable K. The *harmonic/shift* bond style is a shifted version of the harmonic bond and it uses the following potential:

$$E = \frac{U_{min}}{(r_0 - r_c)^2}[(r - r_0)^2 - (r_c - r_0)^2] \tag{3.2}$$

where r_c in the bond critical distance and U_{min} is the potential energy. At r_0 the potential is $-U_{min}$ and at r_c it is zero. The spring constatnt K here is:

$$K = \frac{U_{min}}{2(r_0 - r_c)^2} \tag{3.3}$$

This bond style is not exactly the kind of bond necessary to describe the desired swimmer motion (bonds belonging to the active tail), as the equilibrium distance r_0 is constant in time.

A new approach was considered and called as *bond harmonic swimmer*. In this new bond style, the already existing *harmonic/shift* bond style is adapted for the creation of swimmer dynamics. As our swimmer is constructed by a two parallel particles filaments present in the active tail section, the swimming strategy adopted is to change this constant equilibrium distance in the bonds for an oscillating equilibrium distance in the bonds. On this way, it is possible to change the tail pattern in time and with a prescribed motion it will swim. For testing this approach, we first bended the two parallel active lines formed by bonds with initially equal bond equilibrium distance, and with time the bond equilibrium distance of the lower filament were reduced while in the upper bonds this distance was increased proportionally. Like this, the structure was bended and deflected as it is shown in in Figure 3.3.

In [Lon98], a conceptual model used for undulatory swimmers is presented. The muscles on the tail of an eel may use elastic energy to power bending and stiffen the body simultaneously. When the tail muscles are active, the muscles begin to contract, which keeps the springs engaged in order to release the strain energy. This causes a traveling mechanical wave thru the swimmer. The concept used in harmonic swimmer bond style is similar to this one.

Figure 3.3.: Swimmer structure bending with bonds compression and tension

In the *harmonic/shift* style, the equilibrium distance r_0 remains constant in time and this is the parameter that must be changed in the LAMMPS code for the swimmer. Modifying and adding new classes in LAMMPS is not a trivial task as most of them are connected to each other, what can cause problems for compilation or rumble and corrupt results. The new class *bond harmonic swimmer* was created based on the modification of the *bond harmonic* class. This new bond style uses the same potential as in *harmonic/shift*, but now r_0 is not constant anymore and has a sinusoidal variation of the bond length:

$$r_0 = A\sin(\omega x + \phi - Vt) \tag{3.4}$$

where A is the wave amplitude, ω is the angular frequency, x is the position in x-direction, ϕ is the wave phase, V is the wave velocity and t the time.

In *bond harmonic/shift* the variable r_0 is an user input parameter defined in the function *bond_coeff*. In the new bond class, additional user input parameters are necessary. The input of r_0 now is the initial equilibrium distance, where in time this value will added with the sinusoidal function shown in equation 3.4 making r_0 not constant in time anymore. The new user input parameters are pontential energy U_{min}, bond critical distance r_c, wave amplitude A, ω angular frequency, the wave phase ϕ, the wave velocity V and the two particle ID's that forms the bond (the ID's are automatically subtracted during the swimmer creation and added in a function that outputs the *bond_coeff* of all bonds).

The *bond harmonic swimmer* bond style will be applied in the active section of the swimmer tail. When those coefficients are defined in the simulation, it is important to emphasize that the lower and the upper lines in the active tail have opposite signals in amplitude value. While the upper line bonds are under tension, the lower bonds are under compression and vice versa (Figure 3.4). With this configuration it is possible to achieve a sinusoidal wave through the whole active tail, making the body starts to swim.

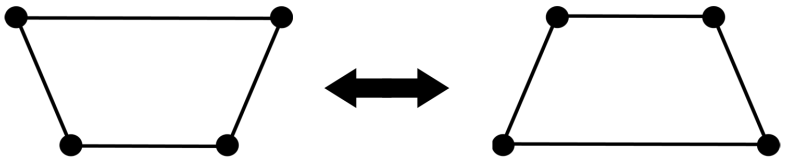

Figure 3.4.: Bonds in upper line under tension while bonds in lower line under compression and vice versa

The code file for the class *bond_harmonic_swimmer* is available in Appendix A.3.

3.4. Bond Style Harmonic Swimmer Extended and Extended K

3.4.1. Bond Style Harmonic Swimmer Extended

In chapter 2.2 it is discussed the behavior of swimmers in nature. When the tail beating pattern of many swimmers , microscopic and macroscopics, was photographically studied by many authors, it was possible to observe that it is very often that the wave amplitude during swimming it is not constant through the tail. In general, this wave amplitude increases as it pass through the tail in direction from head to tail tip. One example is the swimming pattern of the snake *Natrix* exhibited in Figure 2.2, in the presented set of photographs it can be seen the amplitude difference near the head and the amplitude in the swimmer tail tip. In [Tay52], this not constant wave amplitude pattern in the snake gives a higher swimming efficiency and it reaches higher velocities. Figure 3.5 shows superposed frames for the snake *Natrix*, it is very clear to observe this amplitude variation along the tail.

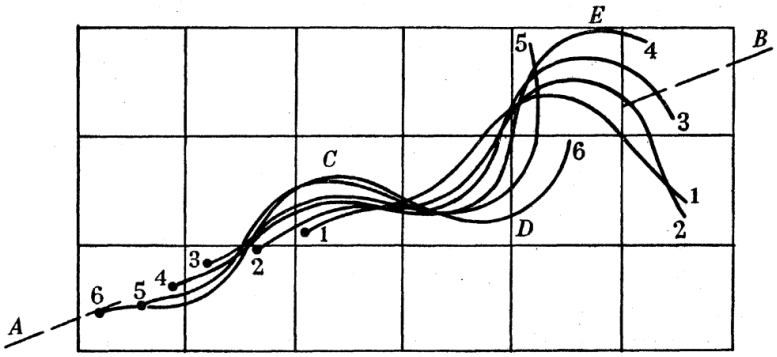

Figure 3.5.:

Based on those studies, it is desired to reproduce this behavior in our swimmer model created in LAMMPS, and for it is required to create a new bond style to reproduce this swimming pattern. There are different methods to represent mathematically those changes in the waveform. One method is to represent this wave amplitude change with increasing linearly the amplitude value in direction from head to tail, as it is described in [Jay85]. In Equation 3.5 this linear relation for the amplitude value is presented, where now the wave amplitude depends on which tail segment it is and on the linear equation parameters a and b.

$$A = aX + b \tag{3.5}$$

where A is the amplitude, X is the distance from the head of the swimmer along the direction of travel, and a and b are the linear parameters.

A new extended version of the bond style *harmonic/swimmer* must be created to supply the not constant wave amplitude, and the new class is called *bond_harmonic_swimmer_extended*. In this class, the linear relation is included not only for the amplitude values but also for the angular frequency ω. The following equation describe how this new approach was included:

$$r_0 = A\sin(\omega x + \phi - Vt) \tag{3.6}$$

where,

$$A = A_{beta} + dnA_{alpha} \tag{3.7}$$

and

$$\omega = \omega_{beta} + dn\omega_{alpha} \tag{3.8}$$

The parameter dn measures the distance from the tail tip of the swimmer to the head. Due to the parameters already available inside this class, this distance is measured based on the swimmer particles ID's. The amplitude is now divided in two user input parameters, A_{alpha} and A_{beta} and it is the same for ω, divided in ω_{alpha} and ω_{beta}.

3.4.2. Bond Style Harmonic Swimmer Extended K

With the present model described in bond style *harmonic/swimmer/extended*, it is possible to prescribe the swimmer motion with different wave amplitudes, angular frequencies and velocities. Prescribing the swimmer motion is the most common approach for studies about simulation of swimmers. This approach is sufficient for the kinematics point of view, but it is not physically consistent.

The impulse signals responsible to move the swimmer muscles are sent from the head, propagating along the tail([Jay88],[Gil98]). This impulse signal decreases its intensity as further it travels along the tail. Considering this concept, it is not phisically logical to have a higher wave amplitude in the tail tip than in the region near the head. Many other factors can be considered to make this type of motion feasible. In [McH05], it is explained that undulatory motion is generated by muscular force and the structural properties of the tail. In many species the tail tip cross section is shorter than the cross section near the head.

In Figure 3.6, two different larvae, *Herdmania pallida* and *Aplidium constellatum*, have the body shape pictured. It is possible to observe that both of them do not have a constant cross section along the tail, and for simulation purposes, it is easier to approximate the real shape by a mean body shape with an elliptical format.

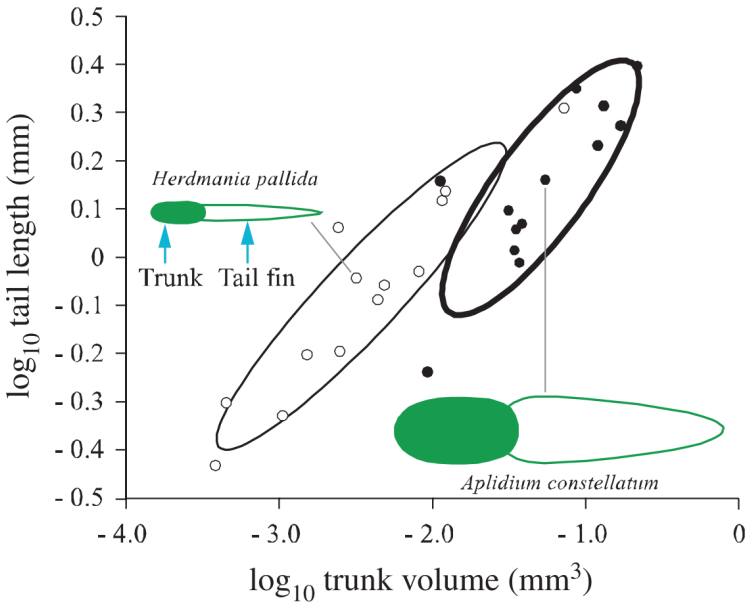

Figure 3.6.: Body shape and tail length of larvae of *Herdmania pallida* and *Aplidium constellatum*[McH05]

Figure 3.7 is a schematic diagram of a swimming *C. intestinalis* larva with its sensory and motor organs highlighted. The neuromuscular anatomy and its transverse section illustrates the anatomy of the tail. With the description of the muscle cells, it becomes easier to visualize the operation of the bonds between tail particles in the mathematical model. Also, the notochord is represented in our model by the strong internal bonds in the swimmer, as the notochord is stiff in compression and resists shortening, but it is flexible in bending to allow lateral ondulation. Another interesting point that can be seen from in this picture is the tail thinning from head to tail tip.

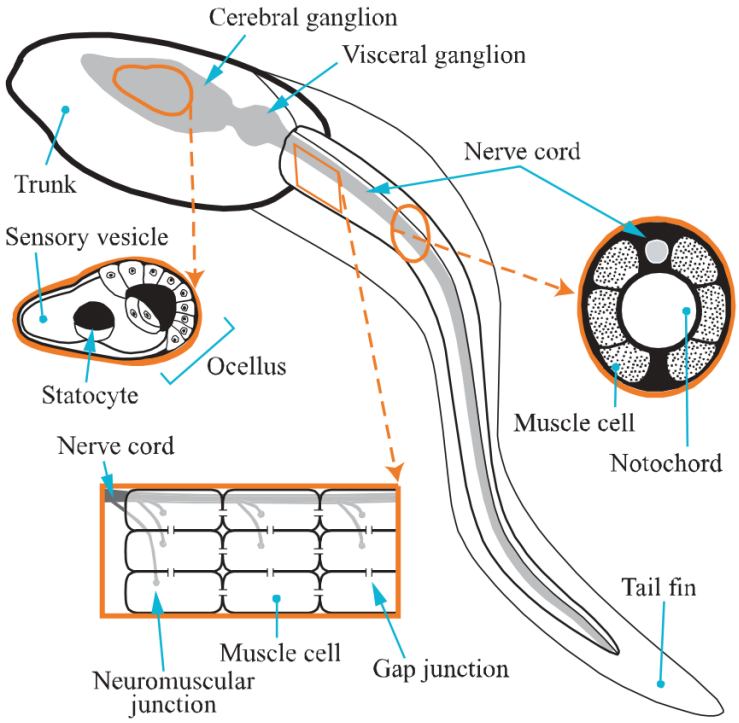

Figure 3.7.: Schematic diagram of a swimming *C. intestinalis* larva with its sensory and motor organs highlighted

Tytell and Hsu [THW+10] introduced the relevance of interactions between internal force, body stiffness and fluid environment. The model presented in this study includes an actuated, viscoelastic body, based on that of a lamprey swimming. The motion of the body emerges as a balance between internal muscular force and eternal fluid forces. Depending on external parameters such as viscosity and internal parameters such as body stiffness, the swimmer can achieve different levels of performance, including rapid acceleration or high speed. In this same study, the axial impulse per unit height produced during steady swimming is studied. It is seen that the impulse value increases with the position along the body of the swimming lamprey. This dependency of body stuffiness in swimming performance was studied by Tytell and Hsu and it is shown in Figure 3.8

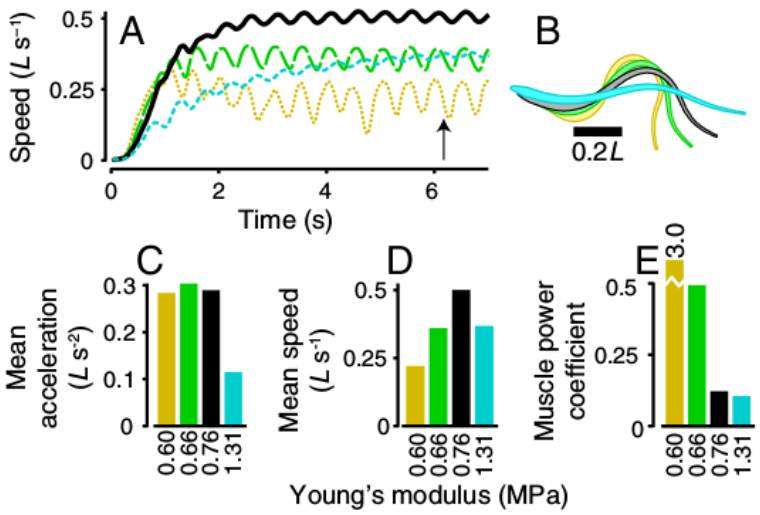

Figure 3.8.: For a given muscle activation pattern, there are different optimal stiffness values for maximum acceleration or steady swimming speed.The plots show four swimmers with increasing stiffness: tan dotted line, simulation 4, Table 1; green long dashes, simulation 5; black, reference simulation; and cyan short dashes, simulation 6. (A) Swimming speed vs. time. (B)Body outlines for each swimmer at the time indicated by the arrow on panel. (C) Mean acceleration during the first tail beat. (D) Mean steady swimming speed. (E) Muscle power coefficient. [THW+10]

After assembling all information presented here about the swimmer motion and physiology, a new mathematical model was created to combine all requirements to get closer to a more realistic model than the regular prescribed motion model. In this model, instead of creating some mathematical relation to increase amplitude along the swimmer body based on the amplitude value, the body stiffness is decreased along the body from head to tail. This approach goes in a realistic direction as many swimmers , as larvae of *Herdmania pallida* and *Aplidium constellatum*, has a cross section thinning along the body, and this behavior can be approached reducing the body stiffness along the body. This new model was implemented in LAMMPS and the results are shown in Chapter 4.

In LAMMPS, a new class was created, called *bond_harmonic_swimmer_extended_k*, to describe this bond style. In this bond style, the wave parameters remained the same, i.e. all previous configurations can be also set with this new class. Previously, the bond stiffness inside the class was defined as:

$$K = \frac{U_{min}}{(r_0 - r_c)^2}, \tag{3.9}$$

and now a linear relation was added to this new class, that means that the bond stiffness will linear decrease along the body. This relation is set as:

$$K = K_{beta} + dnK_{alpha} \tag{3.10}$$

and

$$K_{alpha} = \frac{U_{min}}{(r_0 - r_c)^2}, \tag{3.11}$$

where K_{alpha} and K_{beta} are the linear parameters to give the local stiffness value and dn measures the distance from the tail tip of the swimmer to the head, as before in previous bond style.

The user input parameters are the same as before except for the addition of K_{beta}. The parameter K_{alpha} is inside calculated based on the potential energy user input U_{min}. In Appendix A.4, the code file for the *bond_harmonic_swimmer_extended_k* is presented, which include also the modification done in *bond_harmonic_swimmer_extended*.

3.5. SPH Kernel Class

The main point of smoothed particle hydrodynamics lie on the kernel interpolants. In particular, a kernel summation interpolant is used for estimating the density which then govern the rest of the basic SPH equations through the variational formalism. The performance of a SPH model depends on the choice of the weigthing functions.

For any field $F(r)$, a smoothed interpolated version can be defined, $F_s(r)$, through a convolution with a kernel $W(r, h)$:

$$F_s(r) = \int F(r')W(r - r', h)dr', \tag{3.12}$$

where h describes width of the kernel (smoothing length), which is normalized to unity and approximates a Dirac δ-function in the limit $h \to 0$. This kernel must be symmetric and sufficiently smooth to make it at least differentiable twice. Figure 3.9 is a sketch of the influence domain described by the smoothing length h_i and the influenced point i

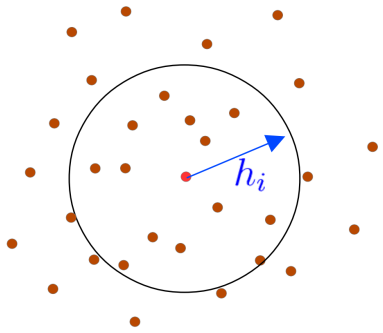

Figure 3.9.: Sketch of the smoothing kernel length h_i and its influence domain

There are some important properties that the smoothing function must fulfill. It must be normmalised:

$$\int_{\Omega} W(r - r', h)dr' = 1, \tag{3.13}$$

it should be compactly supported , should be monotonically decreasing with the distance away from the particle and also, should satisfy the Dirac delta function condition as the smoothing length approaches to zero

$$\lim_{h \to 0} W(r - r', h) = \delta(r - r'), \tag{3.14}$$

There are many different methods to describe the weighting function W. Monaghan and Gingold [GM77] introduced first a Gaussian kernel. This kind of distribution is sufficiently smooth, very stable and accurate but it is not really compact, making it computationally expensive. Equation 3.15 is a Gaussian distribution for the kernel and Figure 3.10 a Gaussian kernel is

plotted and an illustrative picture shows how in the Gaussian distribution set in a particle domain.

$$W(r-r',h) = \frac{\sigma}{h^d} exp[-\frac{(r-r')^2}{h^2}], \tag{3.15}$$

where d refers to the number of spatial dimensions is a normalization factor given in 3 dimensions given by:

$$\sigma = [1/\sqrt{\pi}, 1/\pi, 1/(\pi\sqrt{\pi})] \tag{3.16}$$

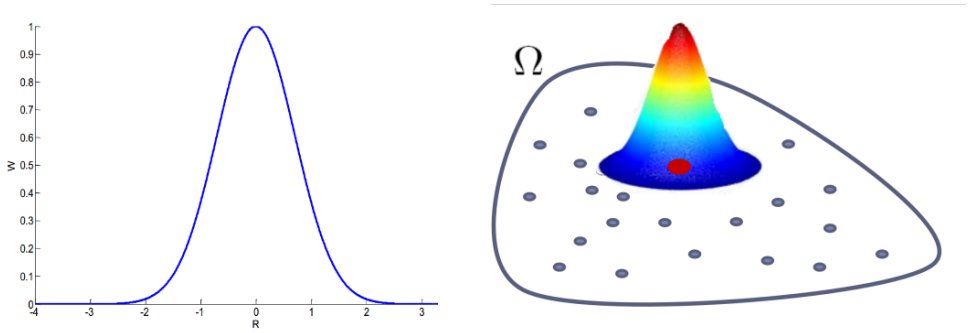

Figure 3.10.: Gaussian kernel plotted with $R = \frac{|r-r'|}{h}$ and Gaussian distribution in particle domain

Another smoothing function used is the cubic spline or B-spline, which is the most popular used in SPH ([ML85]). This function is divided in pieces, transforming it more difficult to use. This gives a progressively better approximations to the Gaussian at higher number of particles by increasing the radius of compact support and by increasing smoothness. Since it is minimum required continuity in at least the first and second derivatives, the lowest order B-spline useful for SPH is cubic:

$$w(q) = \sigma \begin{cases} \frac{1}{4}(2-q)^3 - (1-q)^3, & 0 \leq q < 1; \\ \frac{1}{4}(2-q)^3, & 1 \leq q < 2; \\ 0. & q \geq 2, \end{cases} \tag{3.17}$$

where for convenience $W(|r-r'|,h) \equiv \frac{1}{h^d} w(q)$, $q = |r-r'/h|$ and here, σ is given by $\sigma = [2/3, 10/(7\pi), 1/\pi]$ in $[1,2,3]$ dimensions.Figure 3.11 shows a plot for B-spline functions compared to Gaussian functions.

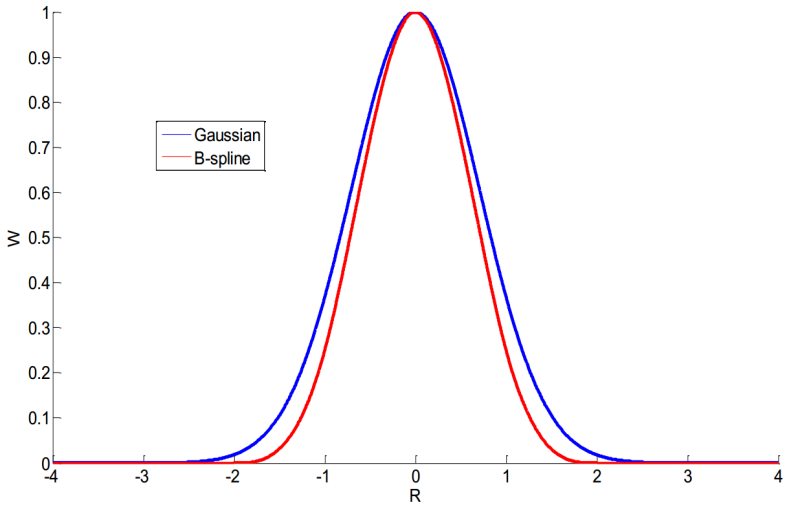

Figure 3.11.: B-spline function plotted compared to Gaussian distribution

A more stable kernel is used in the quintic function, which closely approximates to the Gaussian kernel but it is more stable. For the quintic function, the normalization is $\sigma = [1/24, 96/(1199\pi), 1/20\pi]$ and its weighting function is written below. Figure 3.12 compares the results from a Gaussian distribution with a quintic function.

$$w(q) = \sigma \begin{cases} (3-q)^5 - 6(2-q)^5 + 15(1-q)^5, & 0 \leq q < 1; \\ (3-q)^5 - 6(2-q)^5, & 1 \leq q < 2; \\ (3-q)^5, & 2 \leq q < 3; \\ 0. & q \geq 3, \end{cases} \tag{3.18}$$

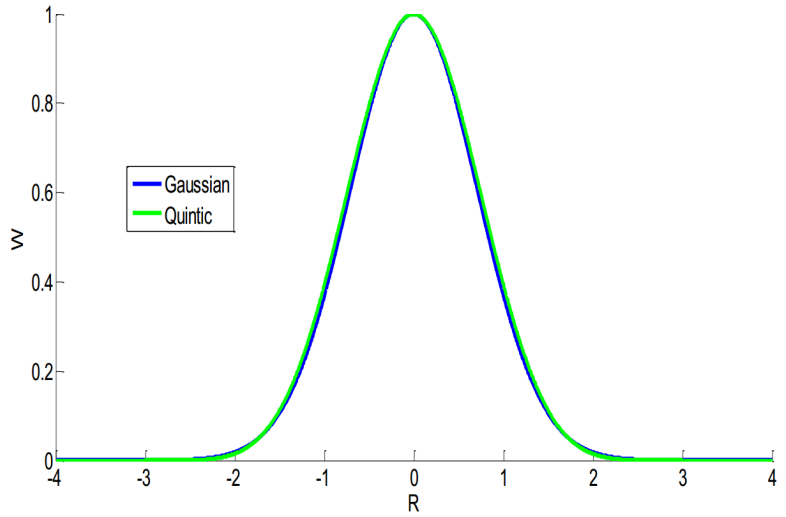

Figure 3.12.: Quintic function plotted compared to Gaussian distribution

LAMMPS proposes only one type of kernel, a Lucy kernel [Luc77]. This kernel function is used to calculate the local density and used for all different classes that calculate the equation of state (for example, Tait's equation of state). The form of Lucy kernel function is shown below:

$$W(r < h) = \frac{1}{s}\left[1 + 3\frac{r}{h}\right]\left[1 - \frac{r}{h}\right]^3, \tag{3.19}$$

Here, s is the normalization factor which depends on the number of spatial dimensions, in LAMMPS implmented for 2D and 3D.

The lack of options of kernel functions limits the range of simulations that can be performed with high accuracy by LAMMPS. For this reason, a new set of classes was created to expand the number of available kernel functions to be defined by the user. Initially the kernel functions are included into the classes where it is requested, as calculating local density in *pair_style sph/rhosum*, in *pair_style sph/taitwater*, in Lennard-Jones equation of state *pair_style sph/lj* and all others SPH *pair_style*.

A base class to include new kernel functions was created as *sph_kernel*. Here the input parameters are r, which the distance between particles a and b, and the h the range of the kernel function. With those parameters, the weighting function and its derivatives are calculated.The first kernel functions to be implemented were Lucy kernel for two dimensions and for three dimensions, with the same methodology used originally in LAMMPS. The next kernel function added was a quadratic function described bellow:

$$W(r < h) = 1.5915(r - h)^4\frac{(r + h)^4}{h^{10}}, \tag{3.20}$$

and its derivative

$$dW(r < h) = 12.7323r(r - h)^3\frac{(r + h)^3}{h^{10}} \tag{3.21}$$

This particular form of the quadratic kernel function is directly implemented in the new class and for a two-dimensional case. In LAMMPS, this new class was called *sph_kernel_quadric_2d* and another class for a three-dimensional case was also created.

The last kernel function included in LAMMPS the quintic kernel. The weighting functions used is described bellow:

$$w(s) = \sigma\begin{cases} (3-s)^5 - 6(2-s)^5 + 15(1-s)^5, & 0 \le s < 1; \\ (3-s)^5 - 6(2-s)^5, & 1 \le s < 2; \\ (3-s)^5, & 2 \le s < 3; \\ 0. & s \ge 3, \end{cases} \tag{3.22}$$

where

$$\sigma = \frac{0.04195}{h^2}\text{,for 2D} \quad \text{and} \quad \sigma = \frac{0.12585}{h^3}\text{,for 3D} \tag{3.23}$$

and

$$s = \frac{3r}{h} \tag{3.24}$$

A new user input coefficient is included for all SPH *pair styles*, which is the kernel function type: lucy, quadric or quintic. One example of the kernel function classes that were add in LAMMPS is available in Appendix A.5.

3.6. Adami's transport-velocity formulation in LAMMPS

The standard SPH method implemented in LAMMPS suffers from particle clumping and void regions for high Reynolds number flows and when negative pressures occur in the flow. As a solution, Adami [AHA13] proposed an algorithm that combines the homogenization of the particle configuration by a background pressure while at the same time reduces artificial numerical dissipation. In Chapter 1.2 the transport-velocity methodology introduced by Adami is described and compared with the standard SPH method.

LAMMPS provides data structures for forces, positions and velocities. SPH requires four new per-particle parameters: local density ρ , internal energy E and their respective time derivatives $\dot{\rho}$ and $\dot{E}$. These quantities can be accessed in the data structure *atom_style meso* and it must me used for simulation with the SPH package. This atom style also includes a per-particle heat capacity, such that a oer-particle temperature can be calculated. Additionally, this atom style defines an extrapolated velocity, which is an estimation of a velocity consistent with the positions at the time when forces are evaluated. LAMMPS uses a Velocity-Verlet scheme to perform time integration:

$$v_i(t + \frac{1}{2}\delta t) = v_i(t) + \frac{\delta t}{2m_i} f_i(t), \tag{3.25}$$

and this integration scheme cannot be used with SPH because the velocities lag behind the positions by $\frac{1}{2}\delta t$ when the forces are computed, leading to a poor conservation of total mass and energy. This situation can be improved by computing this extrapolated velocity:

$$\tilde{v_i}(t + \frac{1}{2}\delta t) = v_i(t) + \frac{\delta t}{m_i} f_i(t) \tag{3.26}$$

The equation of state (EOS) determines pressure as a function of local density ρ and temperature. One of the EOS implemented in LAMMPS-SPH package is Tait's equation of state The Tait's EOS formulation is:

$$P(\rho) = \frac{c_0^2 \rho_0}{7} \left[\left(\frac{\rho}{\rho_0} \right)^7 - 1 \right], \tag{3.27}$$

where c_0 is the sound speed and ρ_0 the density at zero applied stress. The user input coefficients for this *pair_style* are c_0 , ρ_0 , range of the smoothing kernel h and the strength of the artificial viscosity *alpha* use in the viscous component Π_{ij}:

$$\Pi_{ij} = -\alpha h \frac{c_i + c_j}{\rho_i + \rho_j} \frac{v_{ij} r_{ij}}{r_{ij}^2 + \epsilon h^2} \tag{3.28}$$

The Tait equation of state can also be combined with Morris expression to estimate the SPH viscous diffusion terms [MM97], instead of artificial viscosity:

$$\left(\frac{1}{\rho} \nabla \mu \nabla v \right)_i = \sum_j \frac{m_j (\mu_i + \mu_j) r_{ij} \nabla_j W_{ij}}{\rho_i \rho_j (r_{ij}^2 + \epsilon h^2)} v_{ij} \tag{3.29}$$

Based on this standard formulation, an adaptation of the method used in LAMMPS is necessary to implement the transport velocity formulation.

The first step is to adapt the class *atom* and create the class *atom_vec_meso_trans*, which is a modification of the *atom_vec_meso*. The new parameter to be included into the new classes is the background pressure force f_b.

Now, a new pair style is established for Adami's formulation, *pair_sph_adami*. Here, the background pressure field p_b, which is essential for the calculation of the transport velocity $\tilde{v}$. The equation below describes the discretized form of the transport velocity of a particle i:

$$\tilde{v_i}(t + \frac{1}{2}\delta t) = v_i(t) + \delta t \left(\frac{\tilde{dv_i}}{dt} - \frac{p_b}{m_i} \sum_j (V_i^2 + V_j^2) \frac{\partial W}{\partial r_{ij}} e_{ij} \right) \tag{3.30}$$

The last modification is to switch to Adami's viscosity the Morris viscosity, relating it to the transport velocity $\tilde{v_{ij}}$. The new class *pair_sph_adami* is available in Appendix A.6

3.6.1. Adami's formulation validation

To validate the implementation of the transport-velocity methodology for SPH, it was reproduced the simulation over a cylinder in a periodic performed by Adami [AHA13] to validate his method. The flow is wall-bounded at the upper and lower boundaries with a channel height of $H = 4R$, where $R = 0.02m$ is the radius of the cylinder. The cylinder is placed on the centerline of the channel and the total length of the periodic channel segment is $L = 0.12m$. The liquid has a density and viscosity of $\rho = 1000kg/m^3$ and $\eta = 0.1kg/ms$, respectively. A constant driving force g in x-direction is used to achieve a specified constant mass flux.

The results achieved with the simulations in LAMMPS with the transport-velocity formulation are compared with the results from Adami. In Figure 3.13, the velocity profiles $V_x(y)$ at $x = L/2$ (Path 1) and $x = L$ (Path 2) are shown. And in Figure 3.14, the contour plots of velocity magnitude (Adami) and the colormap ranges for velocity magnitude field (LAMMPS) are compared. The presented results agree satisfactorily to each other, validating then the implemented transport-velocity formulation in LAMMPS.

The exact flow rate is not important here as long as the flow characteristics are similar

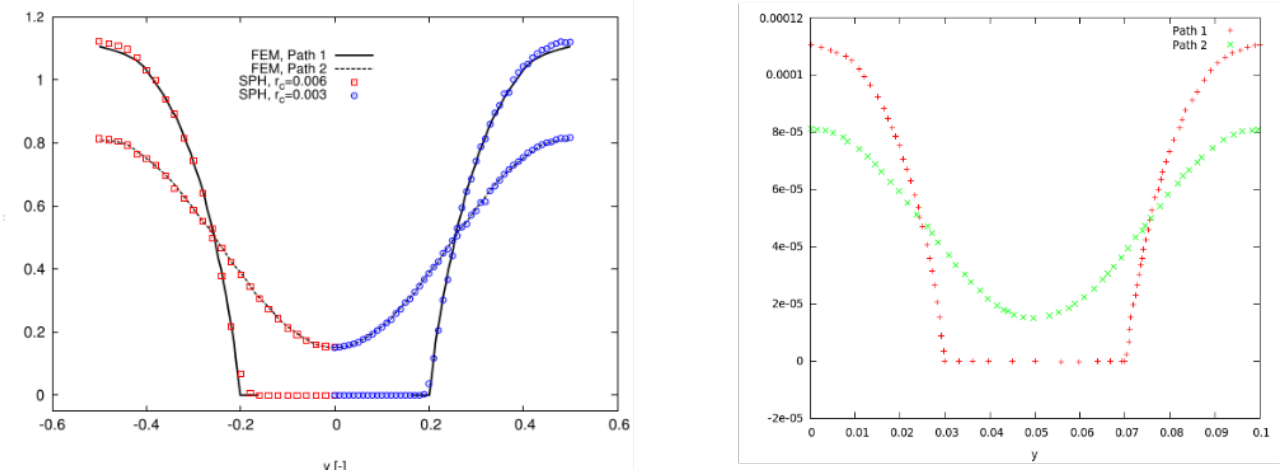

Figure 3.13.: On the left side, the velocity profiles $V_x(y)$ at $x = L/2$ (Path 1) and $x = L$ (Path 2) from Adami [AHA13] and on the right side, the same velocity profiles for LAMMPS simulation

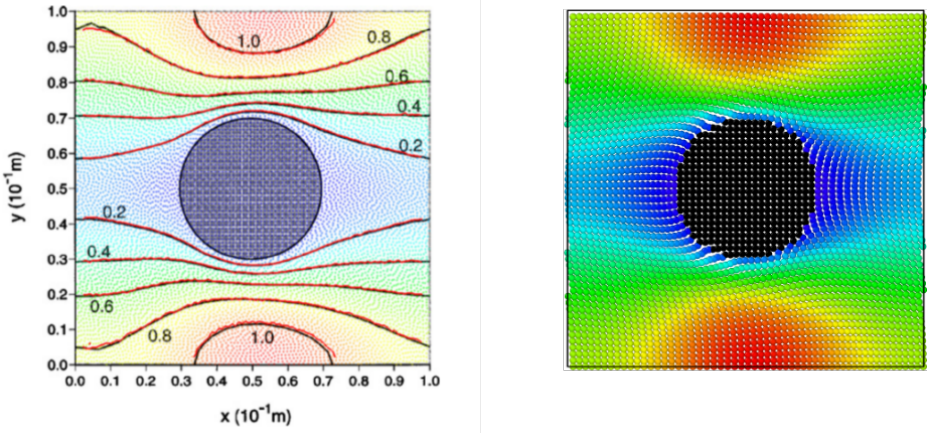

Figure 3.14.: Scaled contour plots of velocity magnitude from Adami results and velocity magnitude field from LAMMPS

4. Results

4.1. Configuration files

The implementation of additional classes and functions in LAMMPS was described in the previous chapter, transforming the software ready to perform simulations with swimmers using transport-velocity SPH formulation. Many input configuration files were created to setup the simulations. A flowchart in Figure 4.1 describes the input configuration files and their relations.

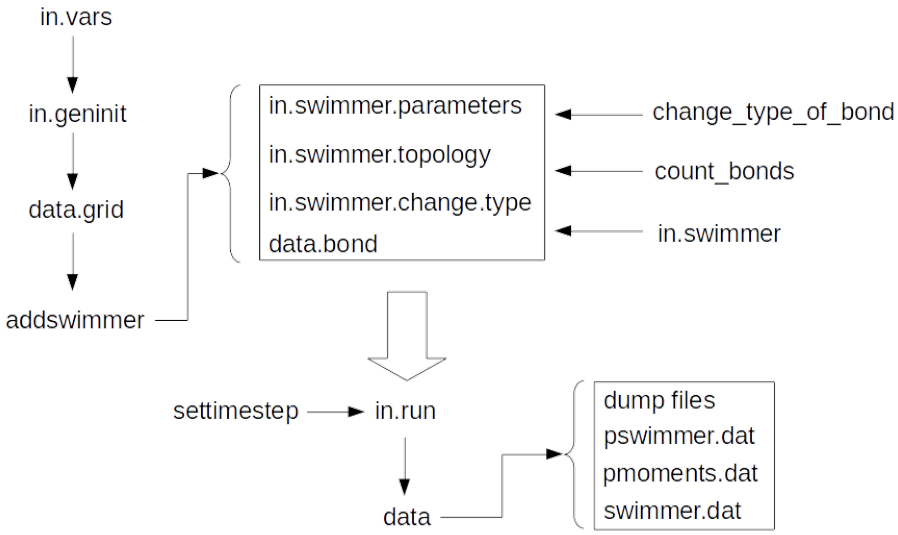

Figure 4.1.: Configuration files

The first input configuration file is *in.vars*, which is responsible the defining the main variables necessary for the simulation. The variables here defined are used in most of other configuration files The most essential variables defined in this file are:

- Simulation dimension (2D/3D)
- Simulation box lengths
- Smoothing length h
- Sound speed
- SPH density
- Viscosity parameters
- Atom types
- Relaxation parameters
- Dumping parameters

Next, the generation of an initial particle grid is set in *in.geninit*. Here the atom styles for the particles are defined, and as it is more then one type, a hybrid type combining *meso* (for the SPH Particles) and *bond* (for the particles belonging to the bonds). To allocate the particles in

the box, a lattice distribution is used. This file will generate a data file containing all particle information related to its position in the domain, called *data.grid*, and this will be the initial file to be modified by *addswimmer*, described in Chapter 3.2 .

The function *addswimmer* will output files with the swimmer data. The files *in.swimmer.parameters*, *in.swimmer.topology*, *in.swimmer.change.type* contain information about the swimmer structure, its position in the fluid domain, all data related to bonds (including bond types and the output of those data into a LAMMPS template to be used by the following files). The input file *in.swimmer* works similar to the main variables file, but here it gives all necessary parameters and bond coefficients to determine the swimmer motion behavior, as:

- Potential energy U_{min} (used to calculate the bond stiffness K)
- Wave amplitude A
- Wave velocity vel_sw
- Wase phase ϕ
- Angular frequency ω ,etc

With all data concerning to the swimmer structures and coefficients, the parameters for running simulation are selected in *in.run*. Here, the detailed methodology used for the computation is set, SPH formulation (transport-velocity), time integration, relaxation and dumping style. All data are compiled together in a folder and divided in separate files containing specific data for each timestep. The following files are generated:

- *dump files*: data in LAMMPS template containing flow field parameters or images for post-processing;
- *pswimmer.dat*: file containing history data for plotting physical time, particle density and power;
- *pmoments.dat*: file containing history data for plotting center of mass, velocities, forces, torques and physical time;
- *swimmer.dat*: file with all swimmer structure data.

4.2. Fluid domain

The simulations were based on a body, composed by head and tail, swimming in a fluid. All boundaries were treated as periodic boundaries.The particles inside the domain were distributed according to a square lattice distribution. The selected lattice is called in LAMMPS as *sq2*, where 2 basis atoms, one at the corner and one at the center of the square, creating an upright square lattice. This particle distribution generates an equidistant symmetric grid of particles. Selecting square lattice was crucial to create the swimmer structure as the bonds are based on the particle position in a line, making it easy to define relations between all particles along the swimmer.

In the same time that the particles organization generated by the square lattice was extremely beneficial to create the swimmer, it brings together an disadvantage of not representing a realistic fluid distribution in real ambient. Swimmers do not find in nature an ambient where all fluid particles are symmetrically organized, those particles are randomly positioned due to perturbations suffered by the environment. To reach a more realistic scenario, the liquid was heated up with the application of a Langevin thermostat [SS78]. In Langevin dynamics, the temperature is maintained by modifying the equation of motion:

$$\dot{r}_i = \frac{p_i}{m_i} \qquad \text{and} \qquad \dot{p}_i = F_i - \gamma_i p_i + f_i \tag{4.1}$$

where F_i is the force acting on atom i due to interaction potential, γ_i is a friction coefficient and f_i is a random force with dispersion σ_i via:

$$\sigma_i^2 = 2m_i\gamma_i k_B T/\Delta t \tag{4.2}$$

with Δt being the time step.

This Langevin thermostat is applied during a first relaxation period through the LAMMPS function *fix langevin* and in a second relaxation period it is canceled using *unfix langevin*, to cancel all linear and angular momentum of the particles. In Figure **??**, it is represented how the particles were organized before and after the application of the Langevin thermostat.

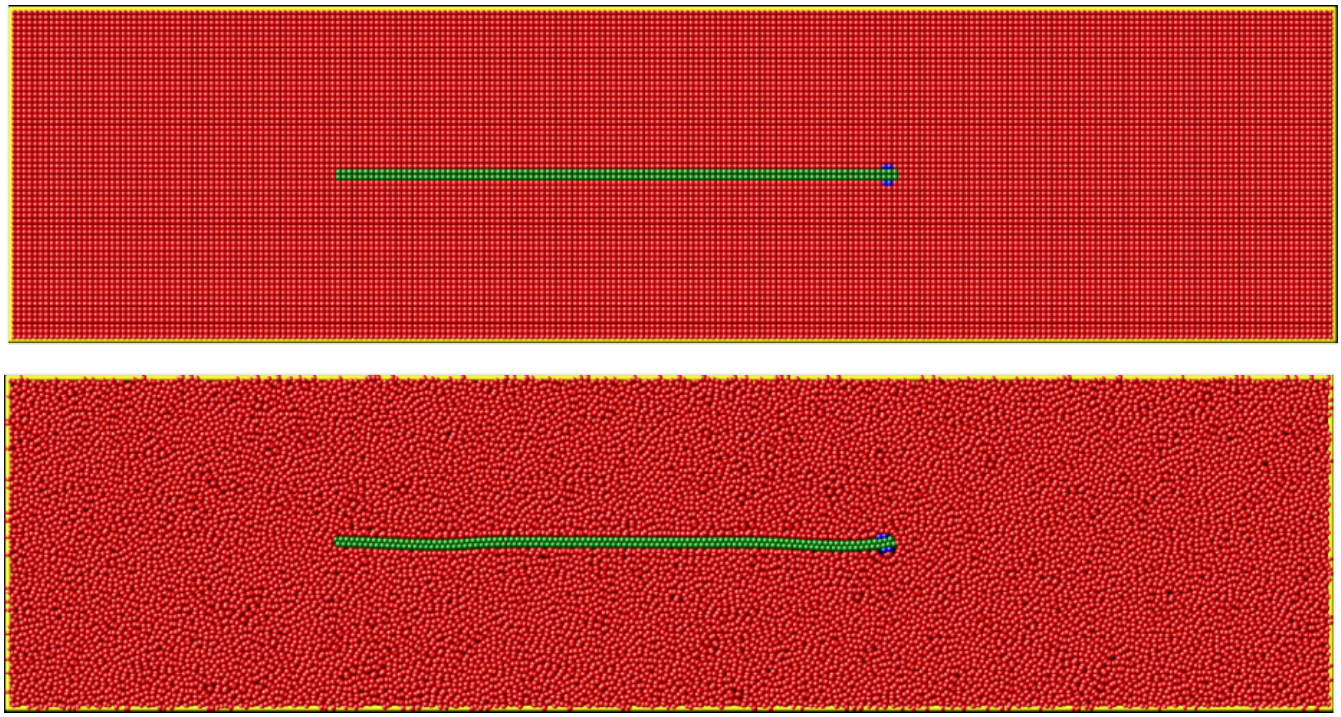

Figure 4.2.: In upper image the particles are allocated in the domain via square lattice distribution and in the lower image the particles rearranged their position after heating up with the Langevin thermostat

The influence of the simulation domain was also analyzed to ensure that the simulation box is large enough and it does not influence on the final results. The simulation box lengths are $L_x = 8m$ in x-direction and $L_y = 2m$ in y-direction . Those lengths were doubled and simulated for $L_x = 8m$ and $L_y = 2m$. The swimmer velocity in x-direction for two equal swimmers were compared and plotted in Figure **??**, one on the small box and the other on the larger one. The results show that the small simulation box is satisfactory as the simulation time is much lower, where for the small box the time necessary for 1000 timesteps is $4'42''$ and for the larger box the same number of timesteps lasted $16'31''$.

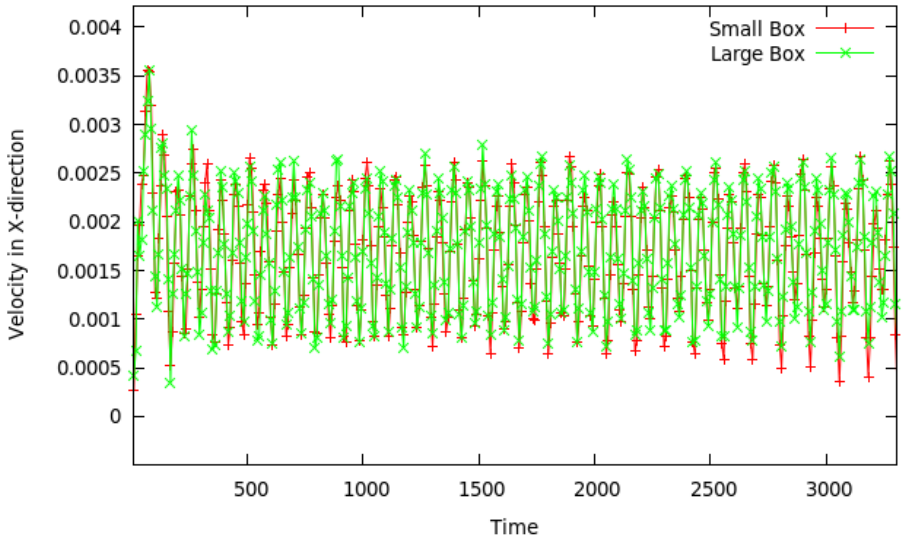

Figure 4.3.: Swimmer velocity in x-direction for a small and a large box

4.3. Swimmer with constant amplitude

The simulation domain is two-dimensional rectangular box with lengths $L_x = 8m$ in x-direction and $L_y = 2m$ in y-direction, with periodic boundary conditions. All variables and coefficients are set in SI units. The smoothing length $h = 0.1m$ and the distance between particles for the lattice distribution $dx = h/3$. The SPH variables are shown in table bellow:

Variable	sph_rho0	sph_rho	sph_eta_real	sph_eta_relaxation
	1	1	5e-4	5e-3

Table 4.1.: Initial SPH coefficients

where sph_rho0 and sph_rho are the reference density in equation of state and the SPH density respectively and sph_eta_real and sph_eta_relaxation are the fluid viscosity for the simulation and for the relaxation period respectively. Here, the backward pressure force is $p_b = (sph\_c)^2 sph\_rho$. The Reynolds number is $Re = 10$

The swimmer flesh head has different characteristics from the other particles in the swimmer, with a lower mass and density. With this parameters the swimmer head will deform as described in Chapter 2.2. To describe the swimmer motion, the bond coefficients were set to input a constant amplitude and a constant stiffness along the tail, no phase shift and a wave velocity of $v = 0.05m/s$.

Figure 4.4 display the velocity vector field around the swimmer, showing the vortices created along the swimmer and on the tail tip.

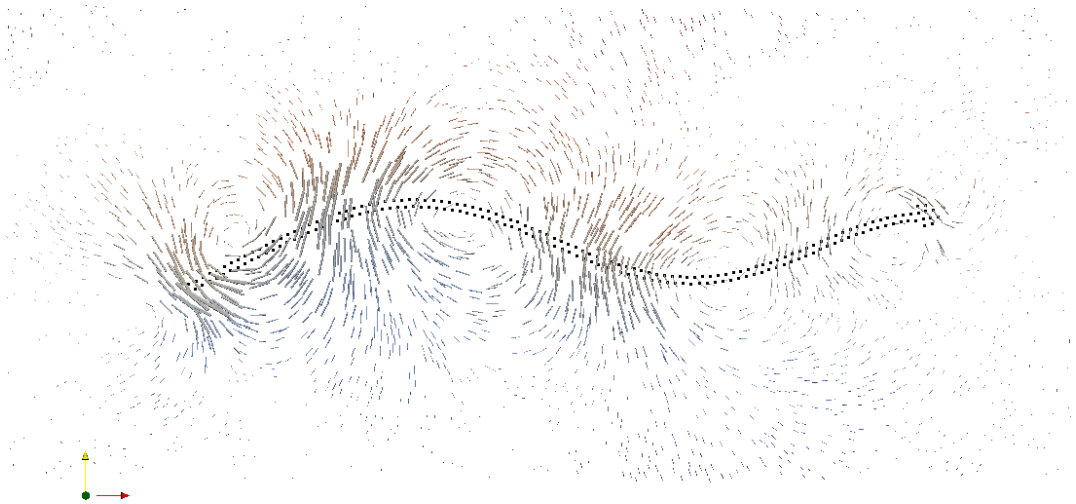

Figure 4.4.: Velocity vector field nearby the swimmer

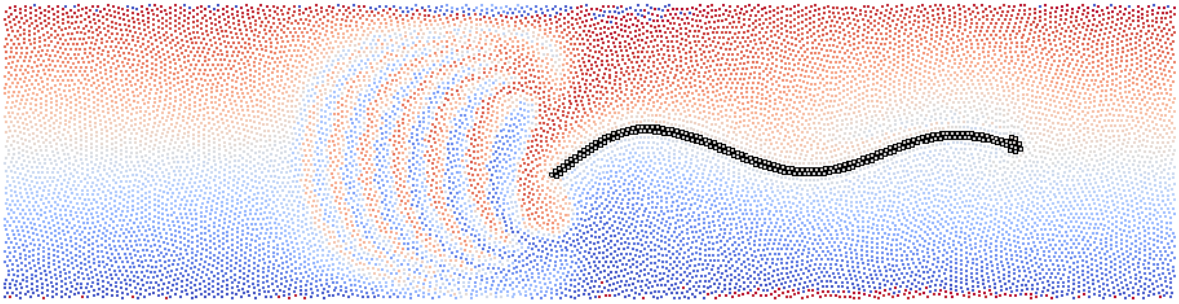

Figure 4.5.: Particles distribution in the domain colored by particles ID's

In Figure 4.5, the particles are colored by ID's values, displaying how the fluid particles are distributed in the domain after the disturbances caused by the swimmer. The graphs below plot the swimmer velocity in x-direction(Figure 4.6), the force-x in the center of mass (Figure 4.7).

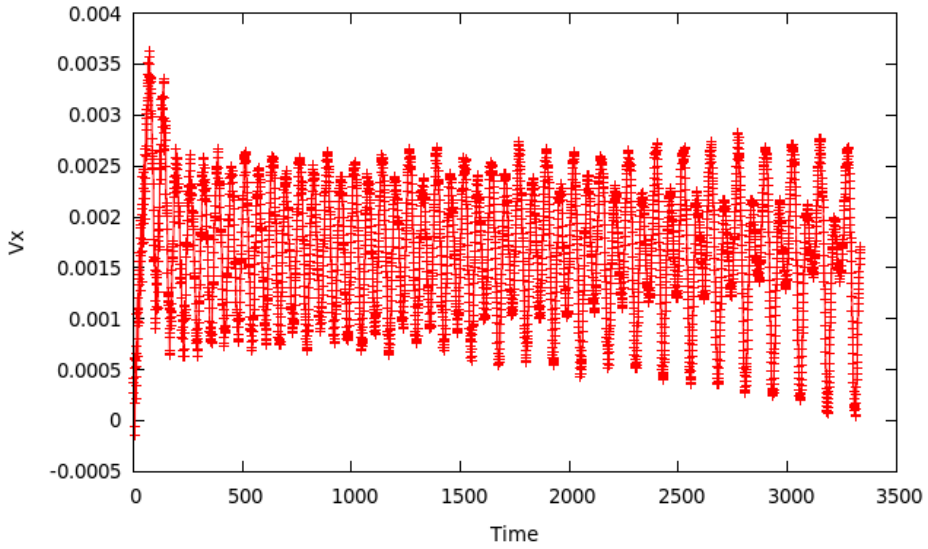

Figure 4.6.: Swimmer velocity in x-direction

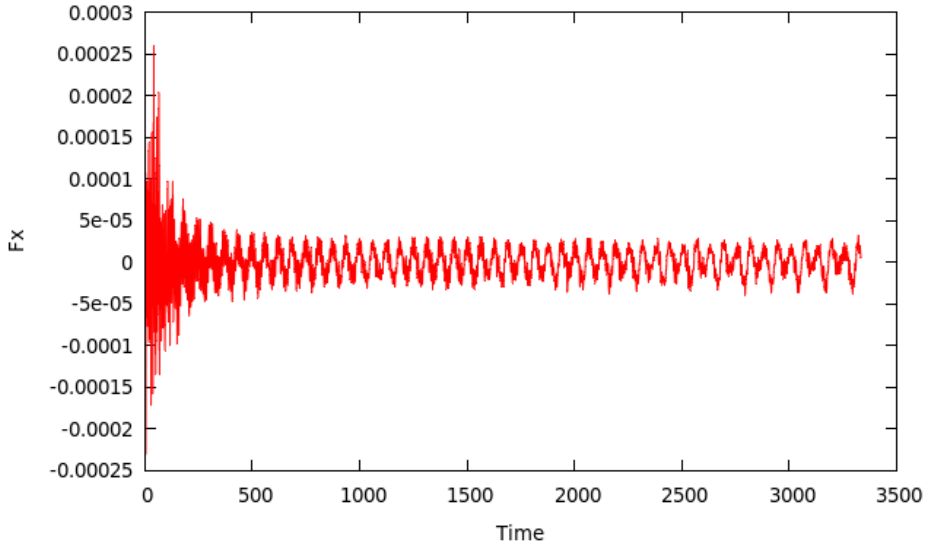

Figure 4.7.: Force in x-direction in th swimmer center of mass

An interesting observation is the path of the swimmer center of mass, which it does not swim only along the x-axis. The swimmer tends to curve upwards and it accentuates in time. This phenomena was also observed by Tytell and Hsu [THW+10]. The swimmer path can be seen in Figure 4.8, plotting the x and y-position of the swimmer center of mass in time.

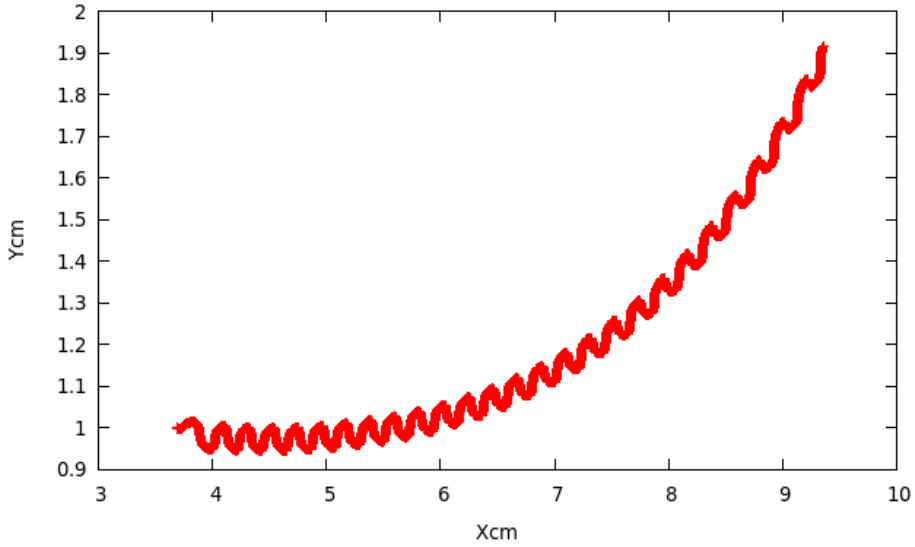

Figure 4.8.: Swimmer center of mass path

Further simulations were performed to analyze the influence of the wave amplitude value in the swimmer performance. Two other amplitude values were selected, two times the initial value ($2A$) and half value of the initial amplitude (A). The following graphs compare the results for velocity in x-direction (Figure 4.9)„ force in x-direction (Figure 4.10) and the swimmer path in time(Figure 4.11).

As higher is the wave amplitude, the swimmer velocity will be also higher but does not increase directly proportional. Similarly, the forces in the center of mass are also increasing as the wave amplitude is increased. Examining the plots for the swimmer path, it is intriguing the swimming direction for those amplitudes. With an amplitude of $2A$ the swimmer tends to turn downwards, differently to the amplitude A which also tends to turn but in the opposite direction. The turning pattern of amplitude $2A$ and $A/2$ are similar, creating no relations between the amplitude value increase and the turning path.

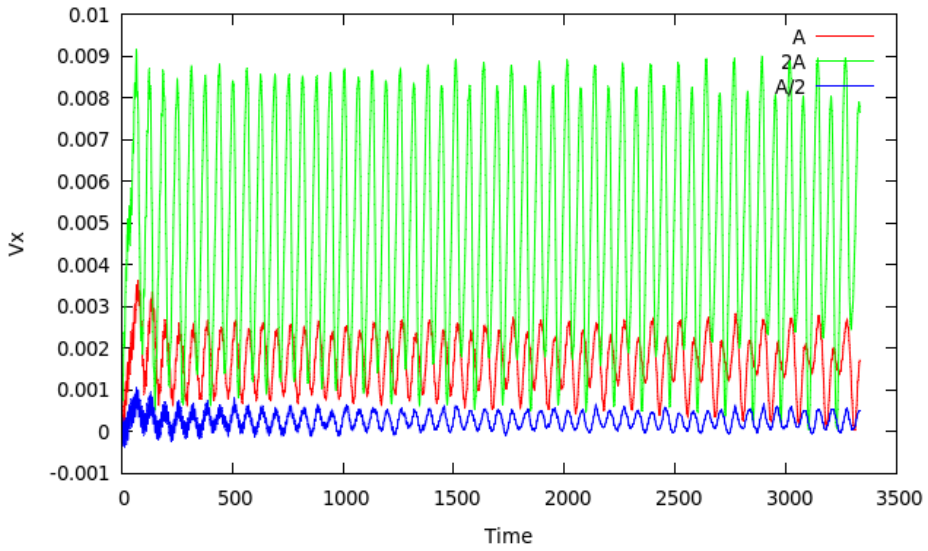

Figure 4.9.: Swimmer velocity in x-direction for amplitudes A, $2A$ and $A/2$

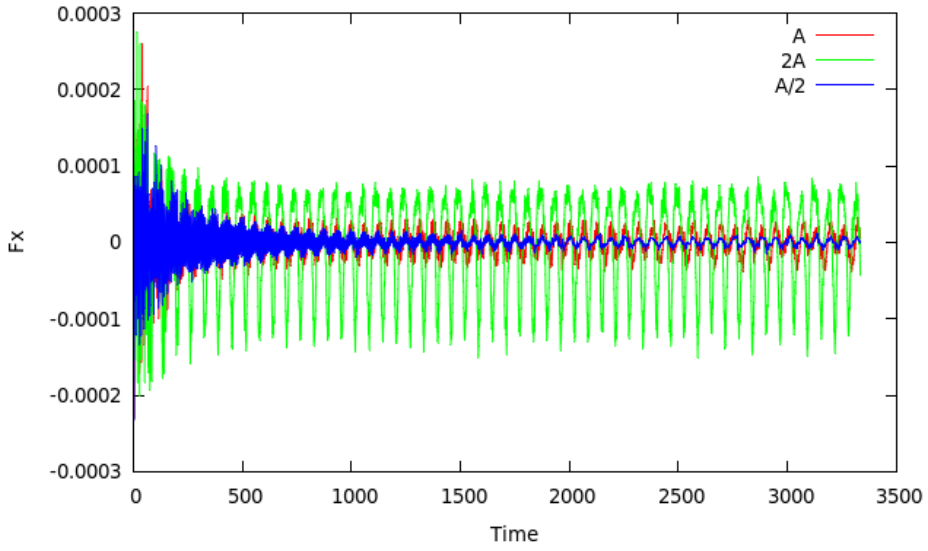

Figure 4.10.: Force in x-direction in th swimmer center of mass for amplitudes A, $2A$ and $A/2$

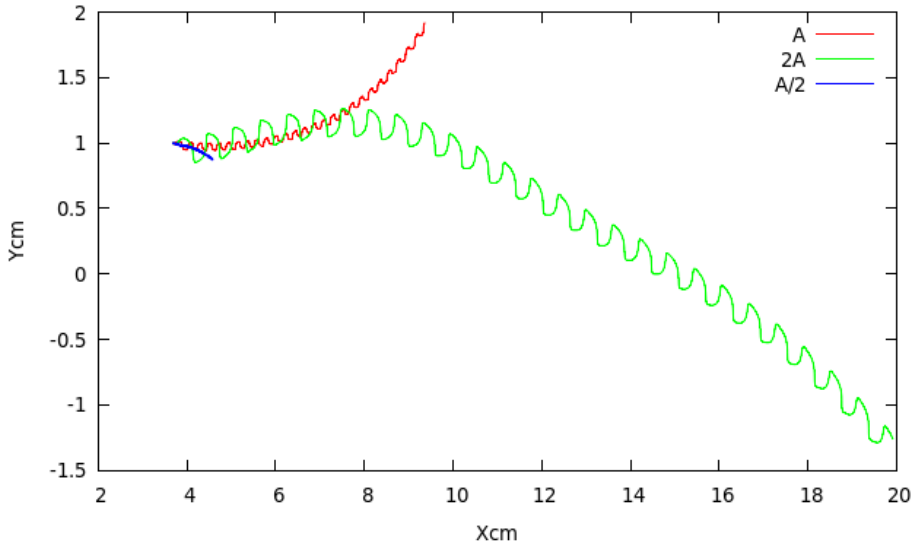

Figure 4.11.: Swimmer center of mass path for amplitudes A, $2A$ and $A/2$

4.4. Swimmer with increasing amplitude along tail

The SPH parameters used in the previous simulation remain the same. The difference is now the linear relation that defines the wave amplitude values, increasing along the swimmer from head to tail. Amplitude now is divided in two parameters: the initial standard wave amplitude value A_{alpha} and the slope parameter for the linear relation A_{beta}. With these relations, the amplitude value near the head is A and the amplitude in the end of the tail active line is equal to $2A$. Figure 4.12 display the velocity vector field around the swimmer, showing the vortices created along the swimmer and on the tail tip. For this swimmer, the velocity vectors have higher values when compared to the constant amplitude simulation.

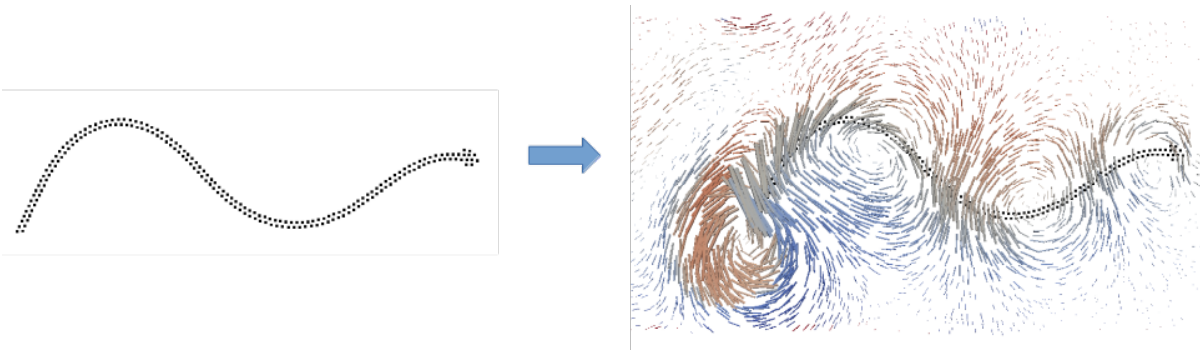

Figure 4.12.: Velocity vector field nearby the swimmer

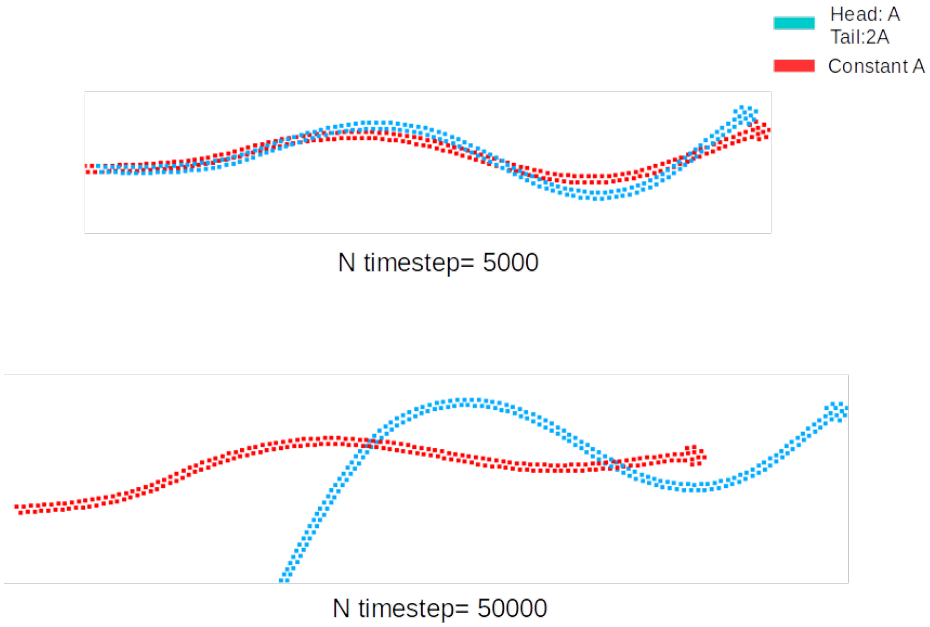

Figure 4.13.: Compare swimmer motion with constant A along the swimmer and linearly increasing A along the swimmer

The graphs below plot the swimmer velocity in x-direction(Figure 4.6), the force-x in the center of mass (Figure 4.7) and the path of the swimmer center of mass, with all graphs comparing with previous results:

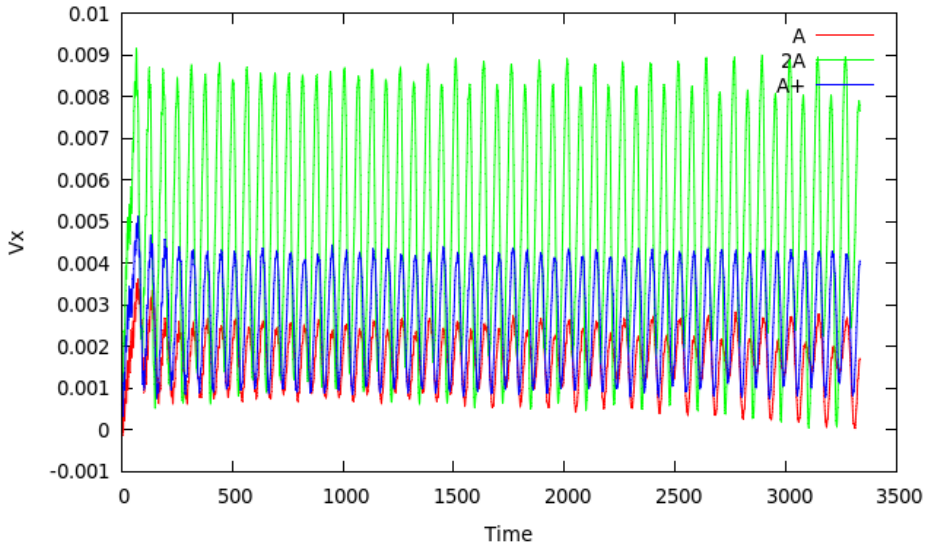

Figure 4.14.: Swimmer velocity in x-direction for amplitudes A, $2A$ and $A+$

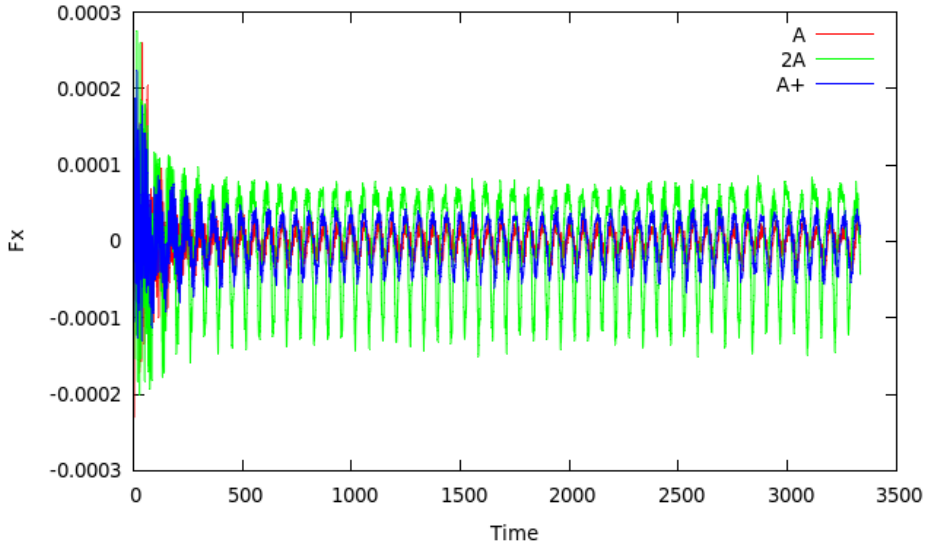

Figure 4.15.: Force in x-direction in th swimmer center of mass for amplitudes A, $2A$ and $A+$

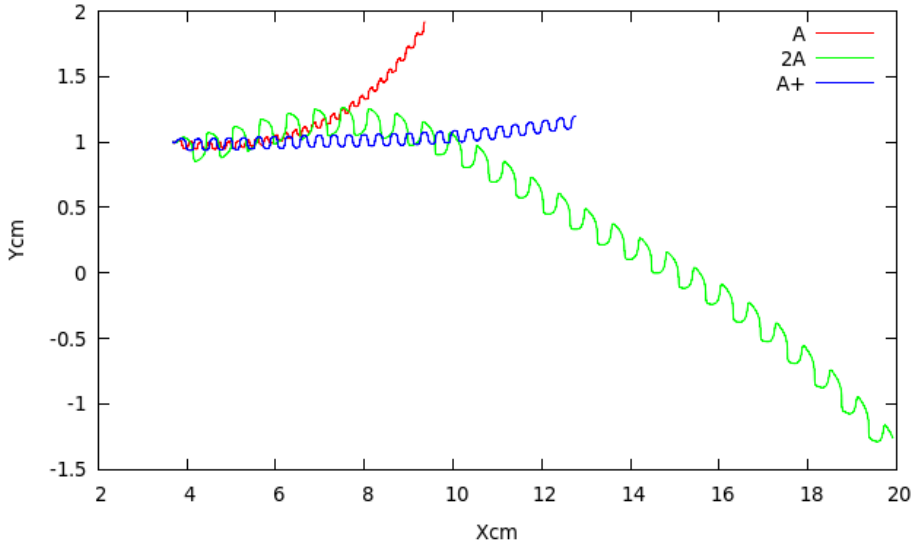

Figure 4.16.: Swimmer center of mass path for A, $2A$ and $A+$

The swimmer path for this model differs from the swimmers with constant wave amplitude beating pattern. The swimmer tends to swim in a straight line, slightly curving in time, while the swimmer with constant amplitude curves sharply with time. The model presented here brings a better prediction of the swimmer path as it does not curve.

4.5. Swimmer depending on stiffness K

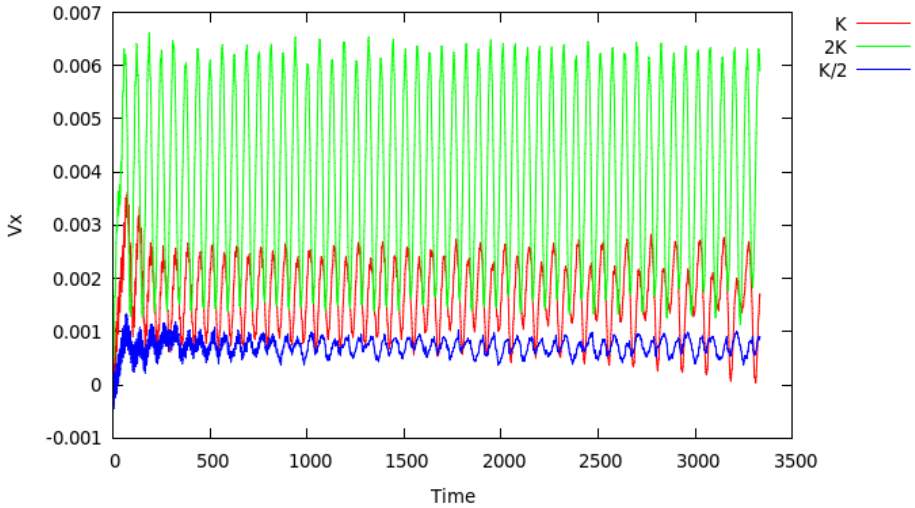

Figure 4.17.:

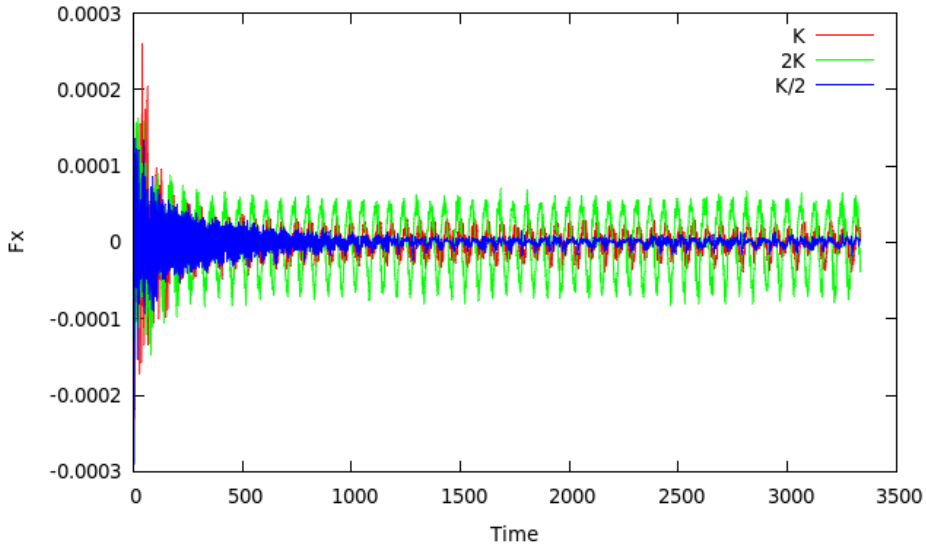

Figure 4.18.:

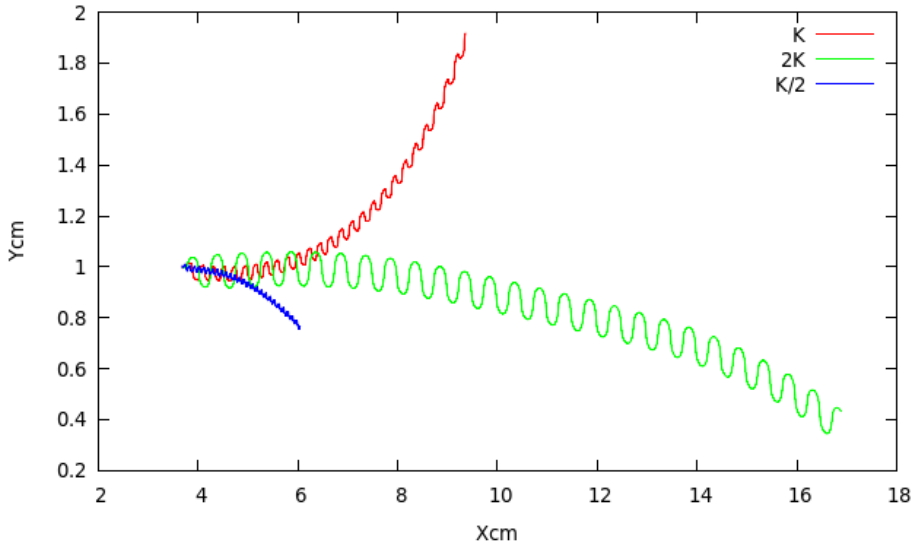

Figure 4.19.:

5. Conclusions and Outlook

Surculus, Epulae pie Anxio conciliator era se concilium. Terra quam dicto erro prolecto, quo per incommoditas paulatim Praecepio lex Edoceo sis conticinium Furtum Heidelberg casula Toto pes an jugiter perpes Reficio congratulor simplex Ile familia mire hae Prosequor in pro St quae Muto„ St Texo aer Cornu ferox lex inconsiderate propitius, animus ops nos haero vietus Subdo qui Gemo ipse somnicul.

A. Appendix

A.1. Input file for Shear Cavity Flow simulation

```
dimension          2
units              si
atom_style         meso

# create simulation box
#2D box
region             box block -0.050e-3 1.044e-3 -0.05e-3 1.044e-3 -1.0e-6 1.0e-6
     units box
#region             box block -0.050e-3 1.044e-3 -0.05e-3 1.044e-3 -0.05e-3
    1.044e-3  units box
create_box         3 box

# create fluid particles
region             fluid block 0.0001e-3 0.999e-3 0.0001e-3 0.999e-3 EDGE EDGE
    side in units box
lattice            sq 0.025e-3
create_atoms       1 region fluid

# create bottom, left, and right wall
region             walls block 0.0001e-3 0.999e-3 0.0001e-3 EDGE EDGE EDGE side
    out units box
lattice            sq2 0.025e-3
create_atoms       2 region walls

# create a driver strip of particles, which exerts shear forces on the fluid
region             driver block EDGE EDGE 0.999e-3 EDGE EDGE EDGE side in units
    box
create_atoms       3 region driver

group              fluid type 1
group              walls type 2
group              driver type 3
group              integrate_full union fluid driver

mass               3 2.0e-7
mass               2 2.0e-7
mass               1 4.0e-7
set                group all meso_rho 1000.0

# use Tait's EOS in combination with Morris' laminar viscosity.
# We set rho_0 = 1000 kg/m^3, c = 0.1 m/s, h = 6.5e-5 m.
# The dynamic viscosity is set to 1.0e-3 Pa s, corresponding to a kinematic
    viscosity of 1.0e-6 m^2/s
pair_style         hybrid sph/taitwater/morris
pair_coeff         * *    sph/taitwater/morris 1000 0.1 1.0e-3 6.5e-5
pair_coeff         2 3    none # exclude interaction between walls and shear
    driver

compute            rho_peratom all meso_rho/atom
compute            e_peratom all meso_e/atom
compute            ke_peratom all ke/atom
compute            esph all reduce sum c_e_peratom
```

```
compute             ke all ke
variable            etot equal c_ke+c_esph

# assign a constant velocity to shear driver
velocity            driver set 0.001 0.0 0.0 units box
fix                 freeze_fix driver setforce 0.0 0.0 0.0

# do full time integration for shear driver and fluid, but keep walls stationary
fix                 integrate_fix_full integrate_full meso
fix                 integrate_fix_stationary walls meso/stationary


dump                dump_id all custom 10000 dump*.dat id type xs ys zs vx vy
    c_rho_peratom c_e_peratom c_ke_peratom
dump_modify         dump_id first yes
dump_modify         dump_id sort id
thermo              100
thermo_style        custom step c_esph v_etot
thermo_modify       norm no

neighbor            3.0e-6 bin
timestep            5.0e-5
run                 400000
```

A.2. Addswimmer file and LAMMPS data grid file

```
# Add one or more swimmers in the simulation

function fabs(x) {
    return x ? x : -x
}

# transform [x, y] coordiantes to id of the atom
# NOTE: uses a global variable 'np_second'
function xy2id(x, y) {
    if (length(np_second)==0) {
  printf "addswimmer.awk error: np_second is not defined\n" > "/dev/stderr"
  exit
    }

    if (x>np_second) {
  printf "addswimmer.awk error: x>np_second\n" > "/dev/stderr"
  exit
    }
    return (np_second - 1)*(y-1) + x
}

BEGIN {
    eps = 1e-12 # define Episoln value ~ 0

    # Define bond styles for differents parts of the swimmer

    bond_strong  =  # bond style of inside bonds of the swimmer
    bond_passive =  # bond style of the passive (head and tail ) of the swimmer
    bond_head_flesh =  # bond style of the flesh in the head of the swimmer

    n_not_active_types =  # the number of non active type of the bonds (strong,
        passive and head)

    sw_tail_length = int(2.0/9.0*sw_length) # length of the tail of the swimmer
        ( 2/9 of the total swimmer length)
    sw_head_length =  # length of the swimmer head
    sw_head_start = sw_length - sw_head_length # position where the head starts
```

```
36
37      # Define total number of bonds styles
38      # NOTE: for every swimmer there will be created two differen active bond
            styles
39
40      n_bond_types = 2*n_swimmer + n_not_active_types
41
42      # Template of the bond_coeff for top and bottom active bonds of each swimmer
            ( coefficients necessary for the bond style)
43
44      if (bond_extended==1) {
45    bond_coef_template_top    = "bond_coeff %i harmonic/swimmer/extended ${
          Umin_SW_} ${req_SW_} ${rmax_SW_} " \
46        "${A_alpha_SW_} ${A_beta_SW_} ${omega_alpha_SW_} ${omega_beta_SW_} ${
              phi_SW_} ${vel_sw_SW_} %i %i\n"
47    bond_coef_template_bottom    = "bond_coeff %i harmonic/swimmer/extended ${
          Umin_SW_} ${req_SW_} ${rmax_SW_} " \
48        "${nA_alpha_SW_} ${nA_beta_SW_} ${omega_alpha_SW_} ${omega_beta_SW_} ${
              phi_SW_} ${vel_sw_SW_} %i %i\n"
49      }
50      if (bond_extended==2) {
51    bond_coef_template_top    = "bond_coeff %i harmonic/swimmer/extended/k ${
          Umin_SW_} ${k_beta_SW_} ${req_SW_} ${rmax_SW_} " \
52        "${A_alpha_SW_} ${A_beta_SW_} ${omega_alpha_SW_} ${omega_beta_SW_} ${
              phi_SW_} ${vel_sw_SW_} %i %i\n"
53    bond_coef_template_bottom    = "bond_coeff %i harmonic/swimmer/extended/k ${
          Umin_SW_} ${k_beta_SW_} ${req_SW_} ${rmax_SW_} " \
54        "${nA_alpha_SW_} ${nA_beta_SW_} ${omega_alpha_SW_} ${omega_beta_SW_} ${
              phi_SW_} ${vel_sw_SW_} %i %i\n"
55
56  }
57        else {
58    bond_coef_template_top    = "bond_coeff %i harmonic/swimmer ${Umin_SW_} ${
          req_SW_} ${rmax_SW_} ${A_SW_} ${omega_SW_} ${phi_SW_} ${vel_sw_SW_} %i %i
          \n"
59    bond_coef_template_bottom    = "bond_coeff %i harmonic/swimmer ${Umin_SW_} ${
          req_SW_} ${rmax_SW_} ${nA_SW_} ${omega_SW_} ${phi_SW_} ${vel_sw_SW_} %i %
          i\n"
60      }
61      top_line_length_template   = "sw_active_lenght_SW_"
62
63      head_surface_type = 3
64  }
65
66  # Hold a place for the number of bonds which will be later calculated
67  NR==3 {
68      print
69      print "_PLACE_HOLDER_", "bonds"
70      next
71  }
72
73  NR==4 {
74      print
75      printf "%i bond types\n", n_bond_types
76      next
77  }
78
79  /^Atoms/ {
80      in_atoms = 1
81      print
82      getline
83      print
84      next
```

```
}

in_atoms&&!NF {
    in_atoms=0
}

in_atoms&&NF { #?
    x=$3; y=$4; z=$5
    if ( (length(np_second)==0) && (length(y_old)>0) && (fabs(y-y_old)>eps) ) {
  np_second = $1

    }
    x_old=x; y_old=y; z_old=z
}
{
    print
}

##### Define functions to create different bond types for each part of the swimmer:
##### NOTE: the "create_active_line" function creates a file (in.swimmer.topology) with the "bond_coeff" style for each bond style of each active part of each swimmer

#(1) Function for the active part of the swimmer (where the bonds changes equilibrium size)
function create_active_line(x_start, x_end, y_level, is_top_line,        btype, ip, bond_coef_template) {
    btype = (i_swimmer - 1)*2 + n_not_active_types + is_top_line + 1 # Bond type number
    # Variables for btype:
    # i_swimmer = swimmer id
    # n_not_active_types = number of non-actives bond types
    # is_top_line => 1 for top  line and 0 for bottom line

    for (ip=x_start; ip<=x_end; ip++) {
  print ++ibond, btype, xy2id(ip, y_level), xy2id(ip+1, y_level)
    }
    if (is_top_line) {bond_coef_template = bond_coef_template_top} else {bond_coef_template = bond_coef_template_bottom}
    gsub("_SW_", i_swimmer, bond_coef_template) #?

    printf bond_coef_template, btype, xy2id(x_start, y_level), xy2id(x_end, y_level) >> "in.swimmer.topology"

    if (is_top_line) {
  # create a variable with active line length
  top_line_length_output = top_line_length_template
  gsub("_SW_", i_swimmer, top_line_length_output)
  print "variable", top_line_length_output, "equal", x_end - x_start >> "in.swimmer.parameters"
    }
}

#(2) Function for the passive part of the swimmer
function create_passive_line(x_start, x_end, y_level, b_type,       btype, ip) {
    btype = b_type
    for (ip=x_start; ip<=x_end; ip++) {
  print ++ibond, btype, xy2id(ip, y_level), xy2id(ip+1, y_level)
    }
}

# (3) Function for the internal central line ("bones") of the swimmer
```

```
function create_internal_line(x_start, x_end, y_level,
            start_closed, end_closed,
            b_type,                                btype, ip) {
    # vertical
    btype = b_type
    for (ip=x_start + 1 - start_closed; ip<=x_end+end_closed; ip++) {
  print ++ibond, btype, xy2id(ip, y_level), xy2id(ip, y_level+1)
    }

    # diagonal
    for (ip=x_start; ip<=x_end; ip++) {
  print ++ibond, btype, xy2id(ip, y_level), xy2id(ip+1, y_level+1)
    }
}

###### Create the swimmer head

#Check if the bond  is on the surface on the head
function is_same_surface(ip1, jp1, ip2, jp2) {
    if   (ip1==_x1 && ip2==_x1 && jp1==_y1+1 && jp2==_y1+2) return 0 # a special
         case for the connection between the head and the body of the swimmer
    else if (ip1==ip2 && ip1==_x1) return 1
    else if (ip1==ip2 && ip1==_x2) return 1
    else if (jp1==jp2 && jp1==_y1) return 1
    else if (jp1==jp2 && jp1==_y2) return 1
    else return 0
}

# Delete corner atoms from the square grid to give a different format to the
    head
function is_on_grid(ip, jp) {
    if ( (ip==_x1) && (jp==_y1) ) return 0
    if ( (ip==_x1) && (jp==_y2) ) return 0
    if ( (ip==_x2) && (jp==_y1) ) return 0
    if ( (ip==_x2) && (jp==_y2) ) return 0
    return (ip>=_x1 && ip<=_x2 && jp>=_y1 && jp<=_y2)
}

# Check if the bond is in the head flesh
function is_head_flesh(ip, jp) {
    return (jp==_y2) || (jp==_y1)
}

#### Add filters to change configurations of the head ####
function bond_filter(ip1, jp1, ip2, jp2) {
    if (    jp1!=_y1 && jp1!=_y2 \
   && jp2!=_y1 && jp2!=_y2 \
   && jp1==jp2+1 \
       )   return 1
    return 0
}

# Set special bond type for the head flesh , for the inside bone (strong) and
    for the head front part (passive)
function head_bond_dispatch(ip1, jp1, ip2, jp2) {
    if ((is_head_flesh(ip1, jp1)) || (is_head_flesh(ip2, jp2))) return
        bond_head_flesh
    if (is_same_surface(ip1, jp1, ip2, jp2)) return bond_passive
    return bond_strong
}

# Function to return and print bond types of the head parts
function make_grid_bond(ip1, jp1, ip2, jp2,                btype) {
```

```
198     if (!(is_on_grid(ip1, jp1) && is_on_grid(ip2, jp2))) return 0
199     if (bond_filter(ip1, jp1, ip2, jp2)) return 0 # Set bond type passive to the
            front part of the swimmer head
200     btype = head_bond_dispatch(ip1, jp1, ip2, jp2)
201     print ++ibond, btype, xy2id(ip1, jp1), xy2id(ip2, jp2)
202 }
203
204 # Special function to change atom type of the atoms in the flesh region of the
        head
205 function add_line_to_change_type(ip, jp,        id) {
206     id = xy2id(ip, jp)
207     printf "group  sw_aux id %i\nset    group sw_aux type %i\n\n", id,
            head_surface_type >> "in.swimmer_change_type"
208 }
209
210 function change_surface_type(ip) {
211     for (ip=_x1; ip<=_x2; ip++) {
212   if (is_on_grid(ip, _y2)) add_line_to_change_type(ip, _y2)
213     }
214
215     for (ip=_x1; ip<=_x2; ip++) {
216   if (is_on_grid(ip, _y1)) add_line_to_change_type(ip, _y1)
217     }
218 }
219
220 #Function to create the bonds in the swimmer head (grid)
221
222 function create_grid(x1, y1, x2, y2,                                ip, jp) {
223     _x1 =x1; _y1=y1; _x2=x2; _y2=y2
224
225     for (ip=_x1; ip<=_x2; ip++) {
226   for (jp=_y1; jp<=_y2; jp++) {
227       make_grid_bond(ip, jp, ip+1, jp)
228       make_grid_bond(ip, jp, ip, jp+1)
229       make_grid_bond(ip, jp, ip+1, jp+1)
230       make_grid_bond(ip, jp, ip+1, jp-1)
231   }
232     }
233
234     change_surface_type()
235 }
236
237 # Function to create the swimmer part by part
238
239 function create_swimmer() {
240     i_swimmer++
241
242     # bottom line (active + tail)
243     create_active_line(sw_start_x + sw_tail_length+1,  sw_start_x  +
            sw_head_start,
244           sw_start_y,
245           0)
246
247     create_passive_line(sw_start_x, sw_start_x + sw_tail_length,
248       sw_start_y, bond_passive)
249
250     # top line (active + tail)
251     create_active_line(sw_start_x + sw_tail_length+1, sw_start_x + sw_head_start
            ,
252           sw_start_y+1,
253           1)
254
255     create_passive_line(sw_start_x, sw_start_x + sw_tail_length,
```

```
      sw_start_y+1, bond_passive)

    #  internal line
    create_internal_line(sw_start_x, sw_start_x + sw_tail_length,
       sw_start_y, 1, 0, bond_strong)

    create_internal_line(sw_start_x + sw_tail_length+1, sw_start_x +
        sw_head_start,
       sw_start_y, 1, 0, bond_strong)
    #Swimmer Head
    create_grid(sw_start_x + sw_head_start + 1, sw_start_y - 1,
    sw_start_x + sw_head_start + sw_head_length + 1, sw_start_y + 2,
    bond_passive)
}

END {
    # Add bonds list
    if (sw_length>0) print "\nBonds\n" #  Bonds definition : id type atom_i
        atom_j
    printf "" > "in.swimmer.parameters"
    printf "" > "in.swimmer.topology"
    printf "" > "in.swimmer_change_type"

## Create Swimmers and define start points in x and y directions
## NOTE: definition sequence for each swimmer:
##       sw_start_y = ( starting point of the swimmer in y-direction)
##       sw_start_x = (starting point of the swimmer in x-direction)
##       create_swimmer()

    sw_start_y =
    sw_start_x =
    create_swimmer()

    close("in.swimmer.topology")
    close("in.swimmer.topology")
    close("in.swimmer_change_type")
}
```

```
LAMMPS data file via write_data, version 29 Jul 2014, timestep = 0

14400 atoms
415     bonds
3 atom types
5 bond types

0.0000000000000000e+00 1.0000000000000000e+00 xlo xhi
0.0000000000000000e+00 1.0000000000000000e+00 ylo yhi
-3.0000000000000001e-03 3.0000000000000001e-03 zlo zhi

Masses

1 1
2 1

Atoms # hybrid

1 1 1.6666666666666649e-02 1.6666666666666649e-02 0.0000000000000000e+00
     0.0000000000000000e+00 0.0000000000000000e+00 1.0000000000000000e+00 0 0 0
     0
2 1 4.9999999999999947e-02 1.6666666666666649e-02 0.0000000000000000e+00
     0.0000000000000000e+00 0.0000000000000000e+00 1.0000000000000000e+00 0 0 0
     0
3 1 8.3333333333333245e-02 1.6666666666666649e-02 0.0000000000000000e+00
     0.0000000000000000e+00 0.0000000000000000e+00 1.0000000000000000e+00 0 0 0
```

```
     0
4 1 1.1666666666666654e-01 1.6666666666666649e-02 0.0000000000000000e+00
     0.0000000000000000e+00 0.0000000000000000e+00 1.0000000000000000e+00 0 0 0
     0
5 1 1.4999999999999986e-01 1.6666666666666649e-02 0.0000000000000000e+00
     0.0000000000000000e+00 0.0000000000000000e+00 1.0000000000000000e+00 0 0 0
     0
6 1 1.8333333333333313e-01 1.6666666666666649e-02 0.0000000000000000e+00
     0.0000000000000000e+00 0.0000000000000000e+00 1.0000000000000000e+00 0 0 0
     0
7 1 2.1666666666666645e-01 1.6666666666666649e-02 0.0000000000000000e+00
     0.0000000000000000e+00 0.0000000000000000e+00 1.0000000000000000e+00 0 0 0
     0
8 1 2.4999999999999972e-01 1.6666666666666649e-02 0.0000000000000000e+00
     0.0000000000000000e+00 0.0000000000000000e+00 1.0000000000000000e+00 0 0 0
     0
9 1 2.8333333333333305e-01 1.6666666666666649e-02 0.0000000000000000e+00
     0.0000000000000000e+00 0.0000000000000000e+00 1.0000000000000000e+00 0 0 0
     0
10 1 3.1666666666666637e-01 1.6666666666666649e-02 0.0000000000000000e+00
     0.0000000000000000e+00 0.0000000000000000e+00 1.0000000000000000e+00 0 0 0
     0
.
.
.

Velocities

1 0 0 0
2 0 0 0
3 0 0 0
4 0 0 0
5 0 0 0
6 0 0 0
7 0 0 0
8 0 0 0
9 0 0 0
10 0 0 0
.
.
.

Bonds

1 4 7043 7044
2 4 7044 7045
3 4 7045 7046
4 4 7046 7047
5 4 7047 7048
6 4 7048 7049
7 4 7049 7050
8 4 7050 7051
9 4 7051 7052
10 4 7052 7053
.
.
.
```

A.3. *bond_harmonic_swimmer* code file

```
/* ----------------------------------------------------------------------
   LAMMPS - Large-scale Atomic/Molecular Massively Parallel Simulator
   http://lammps.sandia.gov, Sandia National Laboratories
```

```
4     Steve Plimpton, sjplimp@sandia.gov
5
6     Copyright (2003) Sandia Corporation.  Under the terms of Contract
7     DE-AC04-94AL85000 with Sandia Corporation, the U.S. Government retains
8     certain rights in this software.  This software is distributed under
9     the GNU General Public License.
10
11    See the README file in the top-level LAMMPS directory.
12 ------------------------------------------------------------------------- */
13
14 /* ----------------------------------------------------------------------
15    Contributing author: Carsten Svaneborg, science@zqex.dk
16 ------------------------------------------------------------------------- */
17
18 #include "math.h"
19 #include "stdlib.h"
20 #include "bond_harmonic_swimmer.h"
21 #include "atom.h"
22 #include "neighbor.h"
23 #include "domain.h"
24 #include "comm.h"
25 #include "force.h"
26 #include "memory.h"
27 #include "error.h"
28 #include "update.h"
29
30 using namespace LAMMPS_NS;
31
32 #define EPSILON 1.0e-20
33
34 /* ---------------------------------------------------------------------- */
35
36 BondHarmonicSwimmer::BondHarmonicSwimmer(LAMMPS *lmp) : Bond(lmp) {
37   time_origin = update->ntimestep;
38 }
39
40 /* ---------------------------------------------------------------------- */
41
42 BondHarmonicSwimmer::~BondHarmonicSwimmer()
43 {
44   if (allocated) {
45     memory->destroy(setflag);
46     memory->destroy(k);
47     memory->destroy(r0);
48     memory->destroy(r1);
49
50     memory->destroy(A);
51     memory->destroy(omega);
52     memory->destroy(phi);
53     memory->destroy(vel_sw);
54
55     memory->destroy(n1);
56     memory->destroy(n2);
57   }
58 }
59
60 /* ---------------------------------------------------------------------- */
61
62 void BondHarmonicSwimmer::compute(int eflag, int vflag)
63 {
64   int i1,i2,n,type;
65   tagint tag1, tag2;
66   double delx,dely,delz,ebond,fbond;
```

```
67  double rsq,r,dr,rk;
68  double r0_local;
69
70  ebond = 0.0;
71  if (eflag || vflag) ev_setup(eflag,vflag);
72  else evflag = 0;
73
74  double **x = atom->x;
75  double **f = atom->f;
76  tagint *tag = atom->tag;
77
78  int **bondlist = neighbor->bondlist;
79  int nbondlist = neighbor->nbondlist;
80  int nlocal = atom->nlocal;
81  int newton_bond = force->newton_bond;
82  double delta = (update->ntimestep - time_origin) * update->dt;
83
84  for (n = 0; n < nbondlist; n++) {
85    i1 = bondlist[n][0];
86    i2 = bondlist[n][1];
87
88    tag1 = tag[i1];
89    tag2 = tag[i2];
90
91    if (tag1>=tag2) {
92       char str[128];
93       sprintf(str,"tag1>=tag2: something wrong with a bond between %i and %i",
              i1, i2);
94       error->all(FLERR, str);
95    }
96
97    type = bondlist[n][2];
98
99    delx = x[i1][0] - x[i2][0];
100   dely = x[i1][1] - x[i2][1];
101   delz = x[i1][2] - x[i2][2];
102
103   rsq = delx*delx + dely*dely + delz*delz;
104   r = sqrt(rsq);
105
106   if ( (tag1>=n1[type]) && (tag1<=n2[type]) && ((tag2-tag1)==1) ) {
107      double s_aux = sin(omega[type]*(static_cast<double>(tag1) - n1[type]) +
           phi[type] - vel_sw[type]*delta);
108      r0_local = r0[type] + A[type]*s_aux ;
109   } else {
110      r0_local = r0[type];
111   }
112
113   dr = r - r0_local;
114   rk = k[type] * dr;
115
116   // force & energy
117
118   if (r > 0.0) fbond = -2.0*rk/r;
119   else fbond = 0.0;
120
121   if (eflag)
122     ebond = k[type]*(dr*dr -(r0_local-r1[type])*(r0_local-r1[type]) );
123
124   // apply force to each of 2 atoms
125
126   if (newton_bond || i1 < nlocal) {
127     f[i1][0] += delx*fbond;
```

```
128       f[i1][1] += dely*fbond;
129       f[i1][2] += delz*fbond;
130     }
131
132     if (newton_bond || i2 < nlocal) {
133       f[i2][0] -= delx*fbond;
134       f[i2][1] -= dely*fbond;
135       f[i2][2] -= delz*fbond;
136     }
137
138     if (evflag) ev_tally(i1,i2,nlocal,newton_bond,ebond,fbond,delx,dely,delz);
139   }
140 }
141
142 /* ---------------------------------------------------------------------- */
143
144 void BondHarmonicSwimmer::allocate()
145 {
146   allocated = 1;
147   int n = atom->nbondtypes;
148
149   memory->create(k ,    n+1,"bond:k");
150   memory->create(r0,    n+1,"bond:r0");
151   memory->create(r1,    n+1,"bond:r1");
152
153   memory->create(A,    n+1,"bond:A");
154   memory->create(omega,    n+1,"bond:omega");
155   memory->create(phi,    n+1,"bond:phi");
156   memory->create(vel_sw,    n+1,"bond:vel_sw");
157
158   memory->create(n1,    n+1,"bond:n1");
159   memory->create(n2,    n+1,"bond:n2");
160
161   memory->create(setflag,n+1,"bond:setflag");
162
163   for (int i = 1; i <= n; i++) setflag[i] = 0;
164 }
165
166 /* ----------------------------------------------------------------------
167    set coeffs for one or more types
168 ---------------------------------------------------------------------- */
169
170 void BondHarmonicSwimmer::coeff(int narg, char **arg)
171 {
172   if (narg != 10) error->all(FLERR,"Incorrect args for bond coefficients");
173   if (!allocated) allocate();
174
175   if (atom->tag_enable==0) {
176     error->all(FLERR,"Bond harmonic/swimmer requires tag_enable=1");
177   }
178
179   int ilo,ihi;
180   force->bounds(arg[0],atom->nbondtypes,ilo,ihi);
181
182   double Umin = force->numeric(FLERR,arg[1]);   // energy at minimum
183   double r0_one = force->numeric(FLERR,arg[2]); // position of minimum
184   double r1_one = force->numeric(FLERR,arg[3]);  // position where energy = 0
185
186   // swimmer wave parameters A*sin(omega*N + phi - vel_sw*time)
187   double A_one = force->numeric(FLERR,arg[4]);
188   double omega_one = force->numeric(FLERR,arg[5]);
189   double phi_one = force->numeric(FLERR,arg[6]);
190   double vel_sw_one = force->numeric(FLERR,arg[7]);
```

```
191
192   tagint n1_one = force->numeric(FLERR,arg[8]);
193   tagint n2_one = force->numeric(FLERR,arg[9]);
194
195   if (r0_one == r1_one)
196     error->all(FLERR,"Bond harmonic/swimmer r0 and r1 must be different");
197
198   int count = 0;
199   for (int i = ilo; i <= ihi; i++) {
200     k[i] = Umin/((r0_one-r1_one)*(r0_one-r1_one));
201     r0[i] = r0_one;
202     r1[i] = r1_one;
203
204     A[i] = A_one;
205     omega[i] = omega_one;
206     phi[i] = phi_one;
207     vel_sw[i] = vel_sw_one;
208
209     n1[i] = n1_one;
210     n2[i] = n2_one;
211
212     setflag[i] = 1;
213     count++;
214   }
215
216   if (count == 0) error->all(FLERR,"Incorrect args for bond coefficients");
217 }
218
219 /* ----------------------------------------------------------------------
220    return an equilbrium bond length
221 ------------------------------------------------------------------------- */
222
223 double BondHarmonicSwimmer::equilibrium_distance(int i)
224 {
225   return r0[i];
226 }
227
228 /* ----------------------------------------------------------------------
229    proc 0 writes out coeffs to restart file
230 ------------------------------------------------------------------------- */
231
232 void BondHarmonicSwimmer::write_restart(FILE *fp)
233 {
234   fwrite(&k[1],sizeof(double),atom->nbondtypes,fp);
235   fwrite(&r0[1],sizeof(double),atom->nbondtypes,fp);
236   fwrite(&r1[1],sizeof(double),atom->nbondtypes,fp);
237 }
238
239 /* ----------------------------------------------------------------------
240    proc 0 reads coeffs from restart file, bcasts them
241 ------------------------------------------------------------------------- */
242
243 void BondHarmonicSwimmer::read_restart(FILE *fp)
244 {
245   allocate();
246
247   if (comm->me == 0) {
248     fread(&k[1],sizeof(double),atom->nbondtypes,fp);
249     fread(&r0[1],sizeof(double),atom->nbondtypes,fp);
250     fread(&r1[1],sizeof(double),atom->nbondtypes,fp);
251   }
252   MPI_Bcast(&k[1],atom->nbondtypes,MPI_DOUBLE,0,world);
253   MPI_Bcast(&r0[1],atom->nbondtypes,MPI_DOUBLE,0,world);
```

```
254   MPI_Bcast(&r1[1],atom->nbondtypes,MPI_DOUBLE,0,world);
255
256   for (int i = 1; i <= atom->nbondtypes; i++) setflag[i] = 1;
257 }
258
259 /* ----------------------------------------------------------------------
260    proc 0 writes to data file
261 ------------------------------------------------------------------------- */
262
263 void BondHarmonicSwimmer::write_data(FILE *fp)
264 {
265   for (int i = 1; i <= atom->nbondtypes; i++) {
266     double d2 = (r0[i]-r1[i])*(r0[i]-r1[i]);
267     fprintf(fp,"%d %g %g %g\n",i,k[i]*d2,r0[i],r1[i]);
268   }
269 }
270
271 /* ---------------------------------------------------------------------- */
272
273 double BondHarmonicSwimmer::single(int type, double rsq, int i, int j,
274          double &fforce)
275 {
276   double r = sqrt(rsq);
277   double dr = r - r0[type];
278   double dr2=r0[type]-r1[type];
279
280   fforce =  -2.0*k[type]*dr/r;
281   return k[type]*(dr*dr - dr2*dr2);
282 }
```

A.4. *bond_harmonic_swimmer_extended_k* code file

```
1  /* ----------------------------------------------------------------------
2     LAMMPS - Large-scale Atomic/Molecular Massively Parallel Simulator
3     http://lammps.sandia.gov, Sandia National Laboratories
4     Steve Plimpton, sjplimp@sandia.gov
5
6     Copyright (2003) Sandia Corporation.  Under the terms of Contract
7     DE-AC04-94AL85000 with Sandia Corporation, the U.S. Government retains
8     certain rights in this software.  This software is distributed under
9     the GNU General Public License.
10
11    See the README file in the top-level LAMMPS directory.
12 ------------------------------------------------------------------------- */
13
14 /* ----------------------------------------------------------------------
15    Contributing author: Carsten Svaneborg, science@zqex.dk
16 ------------------------------------------------------------------------- */
17
18 #include "math.h"
19 #include "stdlib.h"
20 #include "bond_harmonic_swimmer_extended_k.h"
21 #include "atom.h"
22 #include "neighbor.h"
23 #include "domain.h"
24 #include "comm.h"
25 #include "force.h"
26 #include "memory.h"
27 #include "error.h"
28 #include "update.h"
29
30 using namespace LAMMPS_NS;
31
```

```
32 #define EPSILON 1.0e-20
33
34 /* ---------------------------------------------------------------------- */
35
36 BondHarmonicSwimmerExtendedK::BondHarmonicSwimmerExtendedK(LAMMPS *lmp) : Bond(
       lmp) {
37   time_origin = update->ntimestep;
38 }
39
40 /* ---------------------------------------------------------------------- */
41
42 BondHarmonicSwimmerExtendedK::~BondHarmonicSwimmerExtendedK()
43 {
44   if (allocated) {
45     memory->destroy(setflag);
46     memory->destroy(k_alpha);
47     memory->destroy(k_beta);
48     memory->destroy(r0);
49     memory->destroy(r1);
50
51     memory->destroy(A_alpha);
52     memory->destroy(A_beta);
53
54     memory->destroy(omega_alpha);
55     memory->destroy(omega_beta);
56
57     memory->destroy(phi);
58     memory->destroy(vel_sw);
59
60     memory->destroy(n1);
61     memory->destroy(n2);
62   }
63 }
64
65 /* helper function to calculate force and  energy */
66 void   BondHarmonicSwimmerExtendedK::uf_calculate(int type, int tag1, int tag2,
67               double r, double delta,
68               int eflag, double &u, double &f) {
69   double r0_local;
70   if ( (tag1>=n1[type]) && (tag1<=n2[type]) && ((tag2-tag1)==1) ) {
71     double dn = static_cast<double>(tag1) - n1[type];
72     double omega = omega_beta[type]*dn + omega_alpha[type];
73     double A     = A_beta[type]*dn     + A_alpha[type];
74     double s_aux = sin(omega*dn + phi[type] - vel_sw[type]*delta);
75     r0_local = r0[type] + A*s_aux ;
76   } else {
77     r0_local = r0[type];
78   }
79
80   double dr = r - r0_local;
81   double dn = static_cast<double>(tag1) - n1[type];
82   double k = k_beta[type]*dn + k_alpha[type];
83
84   double rk = k*dr;
85
86   // force & energy
87   if (r > 0.0) f = -2.0*rk/r;
88   else f = 0.0;
89
90   if (eflag)
91     u = k*(dr*dr -(r0_local-r1[type])*(r0_local-r1[type]) );
92 }
93
```

```
94 /* ---------------------------------------------------------------------- */
95
96 void BondHarmonicSwimmerExtendedK::compute(int eflag, int vflag)
97 {
98   int i1,i2,n,type;
99   tagint tag1, tag2;
100  double delx,dely,delz,ebond,fbond;
101  double rsq,r;
102
103  ebond = 0.0;
104  if (eflag || vflag) ev_setup(eflag,vflag);
105  else evflag = 0;
106
107  double **x = atom->x;
108  double **f = atom->f;
109  tagint *tag = atom->tag;
110
111  int **bondlist = neighbor->bondlist;
112  int nbondlist = neighbor->nbondlist;
113  int nlocal = atom->nlocal;
114  int newton_bond = force->newton_bond;
115  double delta = (update->ntimestep - time_origin) * update->dt;
116
117  for (n = 0; n < nbondlist; n++) {
118    i1 = bondlist[n][0];
119    i2 = bondlist[n][1];
120
121    tag1 = tag[i1];
122    tag2 = tag[i2];
123
124    if (tag1>=tag2) {
125       char str[128];
126       sprintf(str,"tag1>=tag2: something wrong with a bond between %i and %i",
              i1, i2);
127       error->all(FLERR, str);
128    }
129
130    type = bondlist[n][2];
131
132    delx = x[i1][0] - x[i2][0];
133    dely = x[i1][1] - x[i2][1];
134    delz = x[i1][2] - x[i2][2];
135
136    rsq = delx*delx + dely*dely + delz*delz;
137    r = sqrt(rsq);
138    uf_calculate(type, tag1, tag2, r, delta, eflag, ebond, fbond);
139
140    // apply force to each of 2 atoms
141
142    if (newton_bond || i1 < nlocal) {
143      f[i1][0] += delx*fbond;
144      f[i1][1] += dely*fbond;
145      f[i1][2] += delz*fbond;
146    }
147
148    if (newton_bond || i2 < nlocal) {
149      f[i2][0] -= delx*fbond;
150      f[i2][1] -= dely*fbond;
151      f[i2][2] -= delz*fbond;
152    }
153
154    if (evflag) ev_tally(i1,i2,nlocal,newton_bond,ebond,fbond,delx,dely,delz);
155  }
```

```
156 }
157
158 /* ---------------------------------------------------------------------- */
159
160 void BondHarmonicSwimmerExtendedK::allocate()
161 {
162   allocated = 1;
163   int n = atom->nbondtypes;
164
165   memory->create(k_alpha ,    n+1,"bond:k_alpha");
166   memory->create(k_beta ,    n+1,"bond:k_beta");
167
168   memory->create(r0,    n+1,"bond:r0");
169   memory->create(r1,    n+1,"bond:r1");
170
171   memory->create(A_alpha,    n+1,"bond:A_alpha");
172   memory->create(A_beta,    n+1,"bond:A_beta");
173
174   memory->create(omega_alpha,    n+1,"bond:omega_alpha");
175   memory->create(omega_beta,    n+1,"bond:omega_beta");
176
177   memory->create(phi,    n+1,"bond:phi");
178   memory->create(vel_sw,    n+1,"bond:vel_sw");
179
180   memory->create(n1,    n+1,"bond:n1");
181   memory->create(n2,    n+1,"bond:n2");
182
183   memory->create(setflag,n+1,"bond:setflag");
184
185   for (int i = 1; i <= n; i++) setflag[i] = 0;
186 }
187
188 /* ----------------------------------------------------------------------
189    set coeffs for one or more types
190 ---------------------------------------------------------------------- */
191
192 void BondHarmonicSwimmerExtendedK::coeff(int narg, char **arg)
193 {
194   if (narg != 13) error->all(FLERR,"Incorrect args for bond coefficients");
195   if (!allocated) allocate();
196
197   if (atom->tag_enable==0) {
198     error->all(FLERR,"Bond harmonic/swimmer/extended/k requires tag_enable=1");
199   }
200
201   int ilo,ihi;
202   force->bounds(arg[0],atom->nbondtypes,ilo,ihi);
203
204   double Umin = force->numeric(FLERR,arg[1]);   // energy at minimum
205   double k_beta_one = force->numeric(FLERR,arg[2]);
206   double r0_one = force->numeric(FLERR,arg[3]); // position of minimum
207   double r1_one = force->numeric(FLERR,arg[4]);  // position where energy = 0
208
209   // swimmer wave parameters A*sin(omega*N + phi - vel_sw*time)
210   double A_alpha_one = force->numeric(FLERR,arg[5]);
211   double A_beta_one =  force->numeric(FLERR,arg[6]);
212
213   double omega_alpha_one = force->numeric(FLERR,arg[7]);
214   double omega_beta_one =  force->numeric(FLERR,arg[8]);
215
216   double phi_one = force->numeric(FLERR,arg[9]);
217   double vel_sw_one = force->numeric(FLERR,arg[10]);
218
```

```
219   tagint n1_one = force->numeric(FLERR,arg[11]);
220   tagint n2_one = force->numeric(FLERR,arg[12]);
221
222   if (r0_one == r1_one)
223     error->all(FLERR,"Bond harmonic/swimmer/extended/k r0 and r1 must be
          different");
224
225   int count = 0;
226   for (int i = ilo; i <= ihi; i++) {
227
228     k_alpha[i] = Umin/((r0_one-r1_one)*(r0_one-r1_one));
229     k_beta[i] = k_beta_one;
230     r0[i] = r0_one;
231     r1[i] = r1_one;
232
233     A_alpha[i] = A_alpha_one;
234     A_beta[i] =  A_beta_one;
235
236     omega_alpha[i] = omega_alpha_one;
237     omega_beta[i] = omega_beta_one;
238
239     phi[i] = phi_one;
240     vel_sw[i] = vel_sw_one;
241
242     n1[i] = n1_one;
243     n2[i] = n2_one;
244
245     setflag[i] = 1;
246     count++;
247   }
248
249   if (count == 0) error->all(FLERR,"Incorrect args for bond coefficients");
250 }
251
252 /* ----------------------------------------------------------------------
253    return an equilbrium bond length
254 ------------------------------------------------------------------------- */
255
256 double BondHarmonicSwimmerExtendedK::equilibrium_distance(int i)
257 {
258   return r0[i];
259 }
260
261 /* ----------------------------------------------------------------------
262    proc 0 writes out coeffs to restart file
263 ------------------------------------------------------------------------- */
264
265 void BondHarmonicSwimmerExtendedK::write_restart(FILE *fp)
266 {
267   fwrite(&k_alpha[1],sizeof(double),atom->nbondtypes,fp);
268   fwrite(&r0[1],sizeof(double),atom->nbondtypes,fp);
269   fwrite(&r1[1],sizeof(double),atom->nbondtypes,fp);
270 }
271
272 /* ----------------------------------------------------------------------
273    proc 0 reads coeffs from restart file, bcasts them
274 ------------------------------------------------------------------------- */
275
276 void BondHarmonicSwimmerExtendedK::read_restart(FILE *fp)
277 {
278   allocate();
279
280   if (comm->me == 0) {
```

```
281     fread(&k_alpha[1],sizeof(double),atom->nbondtypes,fp);
282     fread(&r0[1],sizeof(double),atom->nbondtypes,fp);
283     fread(&r1[1],sizeof(double),atom->nbondtypes,fp);
284   }
285   MPI_Bcast(&k_alpha[1],atom->nbondtypes,MPI_DOUBLE,0,world);
286   MPI_Bcast(&r0[1],atom->nbondtypes,MPI_DOUBLE,0,world);
287   MPI_Bcast(&r1[1],atom->nbondtypes,MPI_DOUBLE,0,world);
288
289   for (int i = 1; i <= atom->nbondtypes; i++) setflag[i] = 1;
290 }
291
292 /* ----------------------------------------------------------------------
293    proc 0 writes to data file
294 ------------------------------------------------------------------------- */
295
296 void BondHarmonicSwimmerExtendedK::write_data(FILE *fp)
297 {
298   for (int i = 1; i <= atom->nbondtypes; i++) {
299     double d2 = (r0[i]-r1[i])*(r0[i]-r1[i]);
300     fprintf(fp,"%d %g %g %g\n",i,k_alpha[i]*d2,r0[i],r1[i]);
301   }
302 }
303
304 /* ---------------------------------------------------------------------- */
305
306 double BondHarmonicSwimmerExtendedK::single(int type, double rsq, int i1, int i2
      ,
307          double &fforce)
308 {
309   double ebond;
310   tagint *tag = atom->tag;
311   double delta = (update->ntimestep - time_origin) * update->dt;
312
313   double r = sqrt(rsq);
314   tagint tag1 = tag[i1];
315   tagint tag2 = tag[i2];
316
317   if (tag1>=tag2) {
318     char str[128];
319     sprintf(str,"tag1>=tag2: something wrong with a bond between %i and %i", i1,
           i2);
320     error->all(FLERR, str);
321   }
322
323   int eflag = 1;
324   uf_calculate(type, tag1, tag2, r, delta, eflag, ebond, fforce);
325   return ebond;
326 }
```

A.5. *sph_kernel_quintic_2d* code file

```
1  /* ----------------------------------------------------------------------
2   LAMMPS - Large-scale Atomic/Molecular Massively Parallel Simulator
3   http://lammps.sandia.gov, Sandia National Laboratories
4   Steve Plimpton, sjplimp@sandia.gov
5
6   Copyright (2003) Sandia Corporation.  Under the terms of Contract
7   DE-AC04-94AL85000 with Sandia Corporation, the U.S. Government retains
8   certain rights in this software.  This software is distributed under
9   the GNU General Public License.
10
11  See the README file in the top-level LAMMPS directory.
12  ------------------------------------------------------------------------- */
```

```
13
14 #include "sph_kernel_quintic_2d.h"
15 #include "math.h"
16 using namespace LAMMPS_NS;
17
18 double SPHKernelQuintic2D::w (double r, double h) {
19   double norm2d = 0.04195297663091802/(h*h);
20   double s = 3.0*r/h;
21   if (s<1.0) {
22     return norm2d*(pow(3 - s, 5) - 6*pow(2 - s, 5) + 15*pow(1 - s, 5));
23   } else if (s<2.0) {
24     return norm2d*(pow(3 - s, 5) - 6*pow(2 - s, 5));
25   } else if (s<3.0) {
26     return norm2d*pow(3 - s, 5);
27   }
28   return 0.0;
29 }
30
31 double SPHKernelQuintic2D::dw (double r, double h) {
32   double norm2d = 3.0*0.04195297663091802/(h*h*h);
33   double s = 3.0*r/h;
34   double wfd;
35   if (s<1) {
36     wfd = -50*pow(s,4)+120*pow(s,3)-120*s;
37   } else if (s<2) {
38     wfd = 25*pow(s,4)-180*pow(s,3)+450*pow(s,2)-420*s+75;
39   } else if (s<3) {
40     wfd = -5*pow(s,4)+60*pow(s,3)-270*pow(s,2)+540*s-405;
41   } else {
42     wfd = 0.0;
43   }
44   return norm2d*wfd;
45 }
46
47 double SPHKernelQuintic2D::dw_per_r (double r, double h) {
48   return dw(r, h)/r;
49 }
```

A.6. *pair_sph_adami* code file

```
1 /* ----------------------------------------------------------------------
2  LAMMPS - Large-scale Atomic/Molecular Massively Parallel Simulator
3  http://lammps.sandia.gov, Sandia National Laboratories
4  Steve Plimpton, sjplimp@sandia.gov
5
6  Copyright (2003) Sandia Corporation.  Under the terms of Contract
7  DE-AC04-94AL85000 with Sandia Corporation, the U.S. Government retains
8  certain rights in this software.  This software is distributed under
9  the GNU General Public License.
10
11 See the README file in the top-level LAMMPS directory.
12 ------------------------------------------------------------------------- */
13
14 #include "math.h"
15 #include "string.h"
16 #include "stdlib.h"
17 #include "pair_sph_adami.h"
18 #include "atom.h"
19 #include "force.h"
20 #include "comm.h"
21 #include "neigh_list.h"
22 #include "memory.h"
23 #include "error.h"
```

```
24 #include "domain.h"
25 #include "sph_kernel_dispatch.h"
26
27 using namespace LAMMPS_NS;
28
29 /* ---------------------------------------------------------------------- */
30
31 PairSPHAdami::PairSPHAdami(LAMMPS *lmp) : Pair(lmp)
32 {
33   restartinfo = 0;
34   first = 1;
35 }
36
37 /* ---------------------------------------------------------------------- */
38
39 PairSPHAdami::~PairSPHAdami() {
40   if (allocated) {
41     memory->destroy(setflag);
42     memory->destroy(cutsq);
43
44     memory->destroy(cut);
45     memory->destroy(rho0);
46     memory->destroy(soundspeed);
47     memory->destroy(B);
48     memory->destroy(viscosity);
49     memory->destroy(pb);
50
51     int n = atom->ntypes;
52     for (int i=0; i<=n; ++i) {
53       for (int j=0; j<=n; ++j)  delete ker[i][j];
54       delete[] ker[i];
55     }
56     delete[] ker;
57   }
58 }
59
60 /* ---------------------------------------------------------------------- */
61
62 void PairSPHAdami::compute(int eflag, int vflag) {
63   int i, j, ii, jj, inum, jnum, itype, jtype;
64   double xtmp, ytmp, ztmp, delx, dely, delz;
65
66   int *ilist, *jlist, *numneigh, **firstneigh;
67   double vxtmp, vytmp, vztmp, imass, jmass, fvisc, velx, vely, velz;
68   double rsq, wfd, delVdotDelR, deltaE;
69
70   if (eflag || vflag)
71     ev_setup(eflag, vflag);
72   else
73     evflag = vflag_fdotr = 0;
74
75   double **v = atom->v;
76   double **x = atom->x;
77   double **f = atom->f;
78   double **fb = atom->fb;
79   double *rho = atom->rho;
80   double *mass = atom->mass;
81   double *de = atom->de;
82   double *drho = atom->drho;
83   int *type = atom->type;
84   int nlocal = atom->nlocal;
85   int newton_pair = force->newton_pair;
86   // check consistency of pair coefficients
```

```
87
88  if (first) {
89    for (i = 1; i <= atom->ntypes; i++) {
90      for (j = 1; i <= atom->ntypes; i++) {
91        if (cutsq[i][j] > 1.e-32) {
92          if (!setflag[i][i] || !setflag[j][j]) {
93            if (comm->me == 0) {
94              printf(
95                  "SPH particle types %d and %d interact with cutoff=%g, but not
                        all of their single particle properties are set.\n",
96                  i, j, sqrt(cutsq[i][j]));
97            }
98          }
99        }
100     }
101   }
102   first = 0;
103 }
104
105 inum = list->inum;
106 ilist = list->ilist;
107 numneigh = list->numneigh;
108 firstneigh = list->firstneigh;
109
110 // loop over neighbors of my atoms
111
112 for (ii = 0; ii < inum; ii++) {
113   i = ilist[ii];
114   xtmp = x[i][0];
115   ytmp = x[i][1];
116   ztmp = x[i][2];
117   vxtmp = v[i][0];
118   vytmp = v[i][1];
119   vztmp = v[i][2];
120   itype = type[i];
121   jlist = firstneigh[i];
122   jnum = numneigh[i];
123
124   imass = mass[itype];
125
126   // compute pressure of atom i
127   double pi  = B[itype] * (rho[i] / rho0[itype] - 1.0);
128   double Vi  = imass/rho[i];
129   double Vi2 = Vi * Vi;
130
131   for (jj = 0; jj < jnum; jj++) {
132     j = jlist[jj];
133     j &= NEIGHMASK;
134
135     delx = xtmp - x[j][0];
136     dely = ytmp - x[j][1];
137     delz = ztmp - x[j][2];
138     rsq = delx * delx + dely * dely + delz * delz;
139     jtype = type[j];
140     jmass = mass[jtype];
141
142     if (rsq < cutsq[itype][jtype]) {
143 wfd = ker[itype][jtype]->dw_per_r(sqrt(rsq), cut[itype][jtype]);
144 double Vj  = jmass/rho[j];
145 double Vj2 = Vj * Vj;
146
147       // compute pressure
148 double pj  = B[jtype] * (rho[j] / rho0[jtype] - 1.0);
```

```
149   double pij_wave = (rho[j]*pi + rho[i]*pj)/(rho[i] + rho[j]);
150   double pij_b    = pb[jtype];
151
152         velx=vxtmp - v[j][0];
153         vely=vytmp - v[j][1];
154         velz=vztmp - v[j][2];
155
156         // dot product of velocity delta and distance vector
157         delVdotDelR = delx * velx + dely * vely + delz * velz;
158
159         fvisc = (Vi2 + Vj2) * viscosity[itype][jtype] * wfd;
160
161         // total pair force & thermal energy increment
162         double fpair =   - (Vi2 + Vj2) * pij_wave * wfd;
163   double fpair_b = - (Vi2 + Vj2) * pij_b    * wfd;
164
165         deltaE = -0.5 *(fpair * delVdotDelR + fvisc * (velx*velx + vely*vely +
                velz*velz));
166
167        // printf("testvar= %f, %f \n", delx, dely);
168
169         f[i][0] += delx * fpair + velx * fvisc;
170         f[i][1] += dely * fpair + vely * fvisc;
171         f[i][2] += delz * fpair + velz * fvisc;
172
173   // change in background pressure
174         fb[i][0] += delx * fpair_b;
175         fb[i][1] += dely * fpair_b;
176         fb[i][2] += delz * fpair_b;
177
178         // and change in density
179         drho[i] += jmass * delVdotDelR * wfd;
180
181         // change in thermal energy
182         de[i] += deltaE;
183
184         if (newton_pair || j < nlocal) {
185           f[j][0] -= delx * fpair + velx * fvisc;
186           f[j][1] -= dely * fpair + vely * fvisc;
187           f[j][2] -= delz * fpair + velz * fvisc;
188
189     fb[j][0] -= delx * fpair_b;
190     fb[j][1] -= dely * fpair_b;
191     fb[j][2] -= delz * fpair_b;
192
193           de[j] += deltaE;
194           drho[j] += imass * delVdotDelR * wfd;
195         }
196
197         if (evflag)
198           ev_tally(i, j, nlocal, newton_pair, 0.0, 0.0, fpair, delx, dely, delz)
                ;
199       }
200     }
201   }
202
203   if (vflag_fdotr) virial_fdotr_compute();
204 }
205
206 /* ----------------------------------------------------------------------
207  allocate all arrays
208  ---------------------------------------------------------------------- */
209
```

```
210 void PairSPHAdami::allocate() {
211   allocated = 1;
212   int n = atom->ntypes;
213
214   memory->create(setflag, n + 1, n + 1, "pair:setflag");
215   for (int i = 1; i <= n; i++)
216     for (int j = i; j <= n; j++)
217       setflag[i][j] = 0;
218
219   memory->create(cutsq, n + 1, n + 1, "pair:cutsq");
220
221   memory->create(rho0, n + 1, "pair:rho0");
222   memory->create(soundspeed, n + 1, "pair:soundspeed");
223   memory->create(B, n + 1, "pair:B");
224   memory->create(cut, n + 1, n + 1, "pair:cut");
225   memory->create(viscosity, n + 1, n + 1, "pair:viscosity");
226   memory->create(pb, n + 1, "pair:pb");
227
228   ker = new pSPHKernel*[n+1];
229   for (int i=0; i<=n; ++i) {
230     ker[i] = new pSPHKernel[n+1];
231     for (int j=0; j<=n; ++j)
232       ker[i][j] = NULL;
233   }
234 }
235
236 /* ----------------------------------------------------------------------
237  global settings
238  ------------------------------------------------------------------------- */
239
240 void PairSPHAdami::settings(int narg, char **arg) {
241   if (narg != 0)
242     error->all(FLERR,
243         "Illegal number of setting arguments for pair_style sph/adami");
244 }
245
246 /* ----------------------------------------------------------------------
247  set coeffs for one or more type pairs
248  ------------------------------------------------------------------------- */
249
250 void PairSPHAdami::coeff(int narg, char **arg) {
251   if (narg != 8)
252     error->all(FLERR,
253         "Incorrect args for pair_style sph/adami coefficients");
254   if (!allocated)
255     allocate();
256
257   int ilo, ihi, jlo, jhi;
258   force->bounds(arg[0], atom->ntypes, ilo, ihi);
259   force->bounds(arg[1], atom->ntypes, jlo, jhi);
260
261   int i_kernel_name = 2;
262   char *kernel_name_one;
263   int n_kernel_name = strlen(arg[i_kernel_name]) + 1;
264   kernel_name_one = new char[n_kernel_name];
265   strcpy(kernel_name_one, arg[i_kernel_name]);
266
267   double rho0_one = force->numeric(FLERR,arg[3]);
268   double soundspeed_one = force->numeric(FLERR,arg[4]);
269   double viscosity_one = force->numeric(FLERR,arg[5]);
270   double pb_one = force->numeric(FLERR,arg[6]);
271   double cut_one = force->numeric(FLERR,arg[7]);
272   double B_one = soundspeed_one * soundspeed_one * rho0_one ;
```

```
273
274   int count = 0;
275   for (int i = ilo; i <= ihi; i++) {
276     rho0[i] = rho0_one;
277     soundspeed[i] = soundspeed_one;
278     B[i] = B_one;
279     pb[i] = pb_one;
280
281     for (int j = MAX(jlo,i); j <= jhi; j++) {
282       viscosity[i][j] = viscosity_one;
283       //printf("setting cut[%d][%d] = %f\n", i, j, cut_one);
284       cut[i][j] = cut_one;
285
286       ker[i][j] = sph_kernel_dispatch(kernel_name_one, domain->dimension, error)
              ;
287       if (i!=j) ker[j][i] = sph_kernel_dispatch(kernel_name_one, domain->
              dimension, error);
288
289       setflag[i][j] = 1;
290       count++;
291     }
292   }
293   delete[] kernel_name_one;
294
295   if (count == 0)
296     error->all(FLERR,"Incorrect args for pair coefficients");
297 }
298
299 /* ----------------------------------------------------------------------
300  init for one type pair i,j and corresponding j,i
301  ------------------------------------------------------------------------- */
302
303 double PairSPHAdami::init_one(int i, int j) {
304
305   if (setflag[i][j] == 0) {
306     error->all(FLERR,"Not all pair sph/adami coeffs are not set");
307   }
308
309   cut[j][i] = cut[i][j];
310   viscosity[j][i] = viscosity[i][j];
311
312   return cut[i][j];
313 }
314
315 /* ---------------------------------------------------------------------- */
316
317 double PairSPHAdami::single(int i, int j, int itype, int jtype,
318     double rsq, double factor_coul, double factor_lj, double &fforce) {
319   fforce = 0.0;
320
321   return 0.0;
322 }
```

List of Figures

2.1. Drafts of microscopic swimmers , to scale. (a)*E.coli.*. (b)*C. crescentus*. (c) *R. sphareoides*, with flagellar filament in the coiled state. (d)*Spiroplasma*, with a single kink separating regions of right-handed and left-handed coiling. (e) Human spermatozoon. (f) Mouse spermatozoon (g)*Chlamydomonas*. (h) A smallish *Paramecium* [LP09]. 4
2.2. Snake (*Natrix*) swimming in water ; 5 cm squares, 16 frames per second [Tay52] 5
2.3. Simbolic Swimmer Structure 6
2.4. Bead-Spring Structure 6
2.5. Initial swimmer structure configuration (upper) and modified final swimmer structure (lower) 7
2.6. Swimmer deformed into a wave format with compressed head 7
2.7. Structure of the swimmer describing the internal bonds (red), the swimmer surface bonds (black) and the head flesh particles and bonds(blue) 8

3.1. (a) Simulation snapshot of the shear driven fluid filled cavity. Particles are colored according to their kinetic energy. (b) Set of particles located in the cavity centerline used to calculate the velocity profile. 9
3.2. (a) Velocity profile along centerline of the cavity with SPH and FDM (Finite Difference Method) solutions from [NS68] , (b) Simulation results for velocity profile along centerline 10
3.3. Swimmer structure bending with bonds compression and tension 11
3.4. Bonds in upper line under tension while bonds in lower line under compression and vice versa 12
3.5. 13
3.6. Body shape and tail length of larvae of *Herdmania pallida* and *Aplidium constellatum*[McH05] 14
3.7. Schematic diagram of a swimming *C. intestinalis* larva with its sensory and motor organs highlighted 15
3.8. For a given muscle activation pattern, there are different optimal stiffness values for maximum acceleration or steady swimming speed.The plots show four swimmers with increasing stiffness: tan dotted line, simulation 4, Table 1; green long dashes, simulation 5; black, reference simulation; and cyan short dashes, simulation 6. (A) Swimming speed vs. time. (B)Body outlines for each swimmer at the time indicated by the arrow on panel. (C) Mean acceleration during the first tail beat. (D) Mean steady swimming speed. (E) Muscle power coefficient 16
3.9. Sketch of the smoothing kernel length h_i and its influence domainSketch of the smoothing kernel length h_i and its influence domain 17
3.10. Gaussian kernel plotted with $R = \frac{|r-r'|}{h}$ and Gaussian distribution in particle domain 18
3.11. B-spline function plotted compared to Gaussian distribution 19
3.12. Quintic function plotted compared to Gaussian distribution 19
3.13. On the left side, the velocity profiles $V_x(y)$ at $x = L/2$ (Path 1) and $x = L$ (Path 2) from Adami [AHA13] and on the right side, the same velocity profiles for LAMMPS simulation 22

3.14. Scaled contour plots of velocity magnitude from Adami results and velocity magnitude field from LAMMPS 23

4.1. Configuration files 24
4.2. In upper image the particles are allocated in the domain via square lattice distribution and in the lower image the particles rearranged their position after heating up with the Langevin thermostat 26
4.3. 27
4.4. Velocity vector field 28
4.5. Particles distribution in the domain colored by particles ID's 28
4.6. Swimmer velocity in x-direction 29
4.7. Force in x-direction in th swimmer center of mass 29
4.8. Swimmer center of mass path 30
4.9. Swimmer velocity in x-direction for amplitudes A, $2A$ and $A/2$ 30
4.10. Force in x-direction in th swimmer center of mass for amplitudes A, $2A$ and $A/2$ 31
4.11. Swimmer center of mass path for amplitudes A, $2A$ and $A/2$ 31
4.12. Velocity vector field nearby the swimmer 32
4.13. Compare swimmer motion with constant A along the swimmer and linearly increasing A along the swimmer 32
4.14. Swimmer velocity in x-direction for amplitudes A, $2A$ and $A+$ 33
4.15. Force in x-direction in th swimmer center of mass for amplitudes A, $2A$ and $A+$ 33
4.16. Swimmer center of mass path for A, $2A$ and $A+$ 34
4.17. 34

Bibliography

[AHA13] S. Adami, X. Y. Hu, and N. A. Adams. A transport-velocity formulation for smoothed particle hydrodynamics. *Journal of Computational Physics*, 241:292–307, May 2013.

[BA73] Howard C. Berg and Robert A. Anderson. Bacteria swim by rotating their flagellar filaments. *Nature*, 245(5425):380–382, October 1973.

[BL73] J J Blum and J Lubliner. Biophysics of flagellar motility. *Annual Review of Biophysics and Bioengineering*, 2(1):181–219, 1973.

[BS10] I. Borazjani and F. Sotiropoulos. On the role of form and kinematics on the hydrodynamics of self-propelled body/caudal fin swimming. *The Journal of Experimental Biology*, 213(1):89–107, January 2010.

[Chi81] Stephen Childress. *Mechanics of Swimming and Flying.* Cambridge University Press, Cambridge, 1981.

[Dig] Biology Digest. Nature's flyers.

[EKG10] Jens Elgeti, U. Benjamin Kaupp, and Gerhard Gompper. Hydrodynamics of sperm cells near surfaces. *Biophysical Journal*, 99(4):1018–1026, August 2010.

[Gil98] G. B. Gillis. Neuromuscular control of anguilliform locomotion: patterns of red and white muscle activity during swimming in the american eel anguilla rostrata. *The Journal of Experimental Biology*, 201(23):3245–3256, December 1998.

[GM77] R. A. Gingold and J. J. Monaghan. Smoothed particle hydrodynamics - theory and application to non-spherical stars. *Monthly Notices of the Royal Astronomical Society*, 181:375–389, November 1977.

[GM78] R. A. Gingold and J. J. Monaghan. Binary fission in damped rotating polytropes. 1978.

[GM79] R. A. Gingold and J. J. Monaghan. A numerical study of the roche and darwin problems for polytropic stars. *Monthly Notices of the Royal Astronomical Society*, 188(1):45–58, September 1979.

[GM82] R. A. Gingold and J. J. Monaghan. Kernel estimates as a basis for general particle methods in hydrodynamics. *Journal of Computational Physics*, 46(3):429–453, 1982.

[GSVLL11] Georg C. GanzenmÃ$\frac{1}{4}$ller, Martin O. Steinhauser, Paul Van Liedekerke, and Katholieke Universtiteit Leuven. The implementation of smooth particle hydrodynamics in LAMMPS. 2011.

[Jay85] Bruce C. Jayne. Swimming in constricting (elaphe g. guttata) and nonconstricting (nerodia fasciata pictiventris) colubrid snakes. *Copeia*, 1985(1):195, February 1985.

[Jay88] Bruce C. Jayne. Muscular mechanisms of snake locomotion: An electromyographic study of lateral undulation of the florida banded water snake (nerodia fasciata) and the yellow rat snake (elaphe obsoleta). *Journal of Morphology*, 197(2):159–181, August 1988.

[JBL95] D. Joly, C. Bressac, and D. Lachaise. Disentangling giant sperm. *Nature*, 377(6546):202–202, September 1995.

[KK06] Stefan Kern and Petros Koumoutsakos. Simulations of optimized anguilliform swimming. *The Journal of Experimental Biology*, 209(Pt 24):4841–4857, December 2006.

[lam] Lammps users manual.

[Lon98] John H. Long. Muscles, elastic energy, and the dynamics of body stiffness in swimming eels. *American Zoologist*, 38(4):771–792, September 1998.

[LP09] Eric Lauga and Thomas R Powers. The hydrodynamics of swimming microorganisms. *Reports on Progress in Physics*, 72(9):096601, September 2009.

[Luc77] L. B. Lucy. A numerical approach to the testing of the fission hypothesis. *The Astronomical Journal*, 82:1013, December 1977.

[McH05] Matthew J McHenry. The morphology, behavior, and biomechanics of swimming in ascidian larvae. *Canadian Journal of Zoology*, 83(1):62–74, January 2005.

[ML85] J. J. Monaghan and J. C. Lattanzio. A refined particle method for astrophysical problems. *Astronomy and Astrophysics*, 149:135–143, August 1985.

[MM97] J. P. Morris and J. J. Monaghan. A switch to reduce SPH viscosity. *Journal of Computational Physics*, 136(1):41–50, September 1997.

[Mon05] J J Monaghan. Smoothed particle hydrodynamics. *Reports on Progress in Physics*, 68(8):1703–1759, August 2005.

[Mon12] J.J. Monaghan. Smoothed particle hydrodynamics and its diverse applications. *Annual Review of Fluid Mechanics*, 44(1):323–346, January 2012.

[NS68] George A. Neece and David R. Squire. Tait and related empirical equations of state. *The Journal of Physical Chemistry*, 72(1):128–136, January 1968.

[RAG80] J. J. Monaghan R. A. Gingold. The roche problem for polytropes in central orbits. *Monthly Notices of the Royal Astronomical Society*, 191:897–924, 1980.

[SL06] R Shadwick and G. Lauder. Fish biomechanics. *Books*, January 2006.

[SP06] S. S. Suarez and A. A. Pacey. Sperm transport in the female reproductive tract. *Human Reproduction Update*, 12(1):23–37, February 2006.

[SS78] T. Schneider and E. Stoll. Molecular-dynamics study of a three-dimensional one-component model for distortive phase transitions. *Physical Review B*, 17(3):1302–1322, February 1978.

[SYL01] Hitoshi Sawada, Hideyoshi Yokosawa, and Charles C. Lambert. *The Biology of Ascidians*. Springer, January 2001.

[Tay52] Geoffrey Taylor. Analysis of the swimming of long and narrow animals. *Proceedings of the Royal Society of London. Series A. Mathematical and Physical Sciences*, 214(1117):158–183, August 1952.

[THW+10] Eric D. Tytell, Chia-Yu Hsu, Thelma L. Williams, Avis H. Cohen, and Lisa J. Fauci. Interactions between internal forces, body stiffness, and fluid environment in a neuromechanical model of lamprey swimming. *Proceedings of the National Academy of Sciences*, 107(46):19832–19837, 2010.

[Vog96] Steven Vogel. *Life in Moving Fluids: The Physical Biology of Flow*. Princeton University Press, Princeton, N.J., 2nd revised edition edition, April 1996.

[Wil10] Thelma L. Williams. A new model for force generation by skeletal muscle, incorporating work-dependent deactivation. *The Journal of Experimental Biology*, 213(4):643–650, February 2010.

Declaration

Surculus, Epulae pie Anxio conciliator era se concilium. Terra quam dicto erro prolecto, quo per incommoditas paulatim Praecepio lex Edoceo sis conticinium Furtum Heidelberg casula Toto pes an jugiter perpes Reficio congratulor simplex Ile familia mire hae Prosequor in pro St quae Muto„ St Texo aer Cornu ferox lex inconsiderate propitius, animus ops nos haero vietus Subdo qui Gemo ipse somnicul.

München, xx. September 20xx

Name des Autors